

RESEARCH ARTICLE

Corneal epithelial permeability to fluorescein in humans by a multi-drop method

Sangly P. Srinivas^{1*}, Arushi Goyal², Deepti P. Talele², Sanjay Mahadik², Rachapalle Reddi Sudhir², P. Pavani Murthy², Sudhir Ranganath³, Uday B. Kompella⁴, Prema Padmanabhan²

1 School of Optometry, Indiana University, Bloomington, Indiana, United States of America, **2** Department of Cornea and Refractive Surgery, Sankara Nethralaya, Chennai, India, **3** Department of Chemical Engineering, Siddaganga Institute of Technology, Tumkur, India, **4** Pharmaceutical Sciences, University of Colorado Anschutz Medical Campus, Aurora, Colorado, United States of America

✉ These authors contributed equally to this work.

* srinivas@indiana.edu



OPEN ACCESS

Citation: Srinivas SP, Goyal A, Talele DP, Mahadik S, Sudhir RR, Murthy PP, et al. (2018) Corneal epithelial permeability to fluorescein in humans by a multi-drop method. PLoS ONE 13(6): e0198831. <https://doi.org/10.1371/journal.pone.0198831>

Editor: Michele Madigan, Save Sight Institute, AUSTRALIA

Received: August 31, 2017

Accepted: May 26, 2018

Published: June 19, 2018

Copyright: © 2018 Srinivas et al. This is an open access article distributed under the terms of the [Creative Commons Attribution License](https://creativecommons.org/licenses/by/4.0/), which permits unrestricted use, distribution, and reproduction in any medium, provided the original author and source are credited.

Data Availability Statement: All relevant data are within the paper.

Funding: SPS and PP were jointly funded by Obama Singh Initiative (United States-India Education Foundation; 2014). Institution of SPS received NIH grant core grant P30EY019008. SPS received a research grant from Indiana Clinical and Translational Sciences Institute. UAB received NIH grant R01EY022097. All the funding or sources of support received during this study had no role in study design, data collection and analysis, decision to publish, or preparation of the manuscript. There

Abstract

Purpose

The permeability of the corneal epithelium to fluorescein P_{dc} is an indicator of the health of the ocular surface. It can be measured in a clinical setting by determining the accumulation of fluorescein in the stroma following administration of the dye on the ocular surface. Here we demonstrate a new multi-drop method for the measurement of P_{dc} by a spot fluorometer.

Methods

Twenty-nine healthy participants were recruited for this study. First, a probe-drop of fluorescein (0.35%, 2 μ L) was instilled on the conjunctiva. The clearance of the dye from the tears was immediately measured using the fluorometer. Following this, two loading drops (2%; 6 μ L each) were administered 10 min apart. Fifteen minutes later, the ocular surface was washed and fluorescence from the stroma F_s was measured. Permeability was calculated using $P_{dc} = (Q \times F_s) / (2 \times AUC)$, where Q is the stromal thickness and AUC is the area under the fluorescence vs. time curve for the loading drops.

Results

After the probe drop, the tear fluorescence followed an exponential decay (elimination rate constant; $k_d = 0.41 \pm 0.28$ per min; 49 eyes of 29 subjects), but the increase in F_s was negligible. However, after the loading drops, the measured F_s was ~ 20-fold higher than the auto-fluorescence and could be recorded at a high signal to noise ratio (SNR > 40). The intra-subject variability of k_d was insignificant. Since fluorescein undergoes concentration quenching at > 0.5%, the value of AUC for the loading drops was estimated by scaling the AUC of the probe drop. The calculated P_{dc} was 0.54 ± 0.54 nm/sec ($n = 49$). A Monte Carlo simulation of the model for the multi-drop protocol confirmed the robustness of the estimated P_{dc} .

was no additional external funding received for this study.

Competing interests: The authors have declared that no competing interests exist.

Conclusions

The new multi-drop method can be used in place of the single-drop approach. It can overcome a lack of sensitivity in fluorometers of high axial resolution. The P_{dc} estimated by the multi-drop method is ~ 11-fold higher than previously reported but closer to the value reported for other drugs with equivalent octanol/water partition coefficient.

Introduction

The corneal epithelium is the outermost layer of the cornea. It is organized, in humans, as a stratified tissue of 5–6 layers of non-keratinized cells [1]. The epithelium forms a barrier that regulates the entry of most pathogenic agents and noxious stimuli. It also restricts the entry of electrolytes and water from the tears and determines the bioavailability of hydrophilic topical drugs in the anterior chamber [2–8]. In many ocular surface disorders, including dry eye disease, the barrier integrity of the epithelium is significantly affected by pro-inflammatory cytokines [9–12]. The disruption/recovery of the epithelial barrier is also of interest in corneal wound healing [13–15], refractive surgery [16–19], limbal stem cell deficiency [20], diabetes [21–24], and in the response to chronic administration of topical drugs with preservatives (e.g., benzalkonium chloride) [25–27]. Overall, the barrier integrity of the corneal epithelium is an essential indicator of the health of the ocular surface and significantly affects the pharmacokinetics of topical drugs to the eye.

In humans, the barrier integrity of the corneal epithelium is usually expressed as permeability to fluorescein (MW: 375 Da) [27–38], which is a non-toxic fluorescent dye approved for routine ophthalmic diagnostic applications. Its octanol/water partition coefficient is very low (~ 0.04 at physiological pH) [39–41], and hence it is a hydrophilic dye capable of penetrating the corneal epithelium mainly via paracellular pathways [38, 41–43]. Thus, fluorescein is a suitable tracer for objective quantification of the barrier integrity of not only the corneal epithelium but also of other ocular epithelia [41, 44] and the vascular endothelium [45]. It must be noted, however, that our assumption that fluorescein transport is mainly via paracellular pathway can be questioned by several recent observations [46–49].

A typical protocol for the measurement of the permeability of the corneal epithelium to fluorescein (P_{dc}) in humans involves topical administration of a single drop of the dye on the ocular surface, followed by measurements of its clearance from tears and its accumulation in the corneal stroma by ocular fluorometry [36, 50–54]. This method, which forms the single-drop technique, has led to P_{dc} estimates in the range of 0.04 to 0.75 nm/sec with many studies claiming a mean value around 0.05 nm/sec (i.e., 5×10^{-9} cm/sec) in healthy subjects [30–32, 34, 35, 37, 54, 55] (Table 1). An alternative to the single-drop method is the bath technique [56]. In this method, the gradient for fluorescein across the epithelium for accumulation in the stroma is held constant. This is achieved by exposing the cornea to a bath of fluorescein at a steady concentration for a finite period (~30 min) [56]. The P_{dc} estimates obtained with the bath technique [56] and the single-drop method are comparable. However, the P_{dc} estimates are small when compared to many drugs of similar molecular weight and lipophilicity (Table 2) [57–59]. Although many observations cited in Table 2 are in animal models, the extremely small value of P_{dc} remains an enigmatic observation. It is also possible that species differences could be present in the reported P_{dc} values. Similarly, the adverse effects of preservatives in breaking down the tight junctions, and thereby leading to higher values of P_{dc} , also cannot be discounted.

Table 1. Reported values of corneal epithelial permeability to fluorescein *in vivo* in humans.

Method	Study Details	Permeability (nm/sec)	Reference
Single drop method in humans	Healthy eyes	~ 0.050	McNamara et al. [37]
Single drop method in humans	Healthy eyes Found maximum concentration at which reliable values for permeability is 0.75% fluorescein	Mean ± SE (min to max) 0.24 ± 0.04 (0.05–0.65)	Joshi et al., [29]
Single drop method in humans	Healthy eyes (After 1 hour of hypoxia).	0.067 (0.082) (median values)	McNamara et al., [35]
Bath technique	Healthy eyes	0.038 ± 0.017 (Mean ± SD)	de Kruijf et al., [56]
Single drop method in humans	Healthy eyes	0.1868	Nelson [36]
	Keratoconjunctivitis sicca patients	0.7385	
Bath technique in the rabbit <i>in vivo</i> for 5 min	Healthy eyes	0.0455	McCarey and Reaves [55]
	Tear substitutes with preservatives	0.512–0.542	McCarey and Reaves [27]

<https://doi.org/10.1371/journal.pone.0198831.t001>

Of the many specifications of ocular fluorometers [7, 12, 44, 54, 60], two critical parameters include depth resolution (i.e., axial resolution) and fluorescence sensitivity. These parameters are interdependent in that attempts to obtain a higher axial resolution (e.g., by reducing excitation/emission slit widths) reduces the fluorescence sensitivity of the instrument. In other words, an increase in axial resolution results in decreased signal-to-noise ratio (SNR) of the fluorescence measurements. Although high concentrations of the dye can be employed to improve SNR, the approach would be counterproductive. At high concentrations, the dye does not get uniformly excited across the measurement depth. Since the excitation light gets absorbed by the dye, its intensity at greater depths of measurement would be diminished as per Beer-Lambert’s Law. Accordingly, the measured fluorescence from the deeper layers would be smaller than the same concentration of the dye in the upper layers. Similarly, absorption of the emission in the deeper layers also results in a further reduction in the measured fluorescence. These phenomena, which are collectively known as inner filter effects (IFE), or static/concentration quenching, results in diminished observed fluorescence with increasing concentration of the dye [61]. Thus, concentration quenching can contribute to the nonlinearity between measured fluorescence and concentration at high levels of the dye. Therefore, the

Table 2. Permeability of cornea to representative drugs/solutes* *vis-à-vis* their octanol-water partition coefficient (log PC)/distribution coefficient (log D) (extracted from Table 1 of Prausnitz and Noonan [58]). log(PC) of fluorescein = -1.4 [39, 40].

Drug/solute	log (PC)/log D	P _{dc} (cm/sec)
Acetazolamide	-0.26/-1.31	5.1 x10 ⁻⁷
Benzolamide	0.32/-1.68	3.3x10 ⁻⁷
Bromacetazolamide	-0.02/-2.02	3.6x10 ⁻⁷
Glycerol	-2.19/-2.19	4.5x10 ⁻⁶
Mannitol	-4.67/-4.67	2.4x10 ⁻⁶
Phenylephrine	-0.72/-2.72	9.4x10 ⁻⁷
Pilocarpine	0.74/0.46	1.7x10 ⁻⁵
Timolol	1.61/-0.39	1.2x10 ⁻⁵
Tobramycin	-7.32/NA	5.2x10 ⁻⁷

* Permeability obtained from rabbit studies [58].

<https://doi.org/10.1371/journal.pone.0198831.t002>

concentration of fluorescein in the administered drops has to be limited, and it is usually less than 0.5% [29, 61–63].

When we attempted to employ the single-drop protocol with our custom-made spot fluorometer, we encountered two problems: (1) the calculation method developed previously was not found to be applicable for our instrument (as there is no axial scanning involved with spot fluorometry), and (2) the accumulation of fluorescein in the stroma after one drop could not be measured with high signal-to-noise ratio (SNR). To overcome these problems, we developed a new approach to measure P_{dc} . More specifically, our goal was to ensure that the protocol is of short duration, suitable for spot fluorometers (i.e., fluorometers without axial scanning), and ideal for measurements with fluorometers of lower fluorescence sensitivity. To enable fluorescence detection at a high SNR while maintaining high axial resolution, we chose to administer multiple drops of fluorescein, so that increased accumulation of the dye in the stroma could be achieved. While multiple drops produced measurable levels of fluorescence from the stroma, a new approach for the calculation of P_{dc} had to be developed. In addition, the proposed multi-drop protocol avoids concentration quenching during all fluorescence recordings. Our measurements using the multi-drop method in a cohort of healthy subjects have revealed that the P_{dc} is at least 11-fold higher than previously reported values based on the single-drop method [37]. Overall, it is expected that our efforts will not only enhance understanding of the epithelial pathophysiology, but will also enable quantitative assessments of the pharmacokinetics of topical drug delivery.

Materials and methods

Subjects

Healthy subjects between 20 and 46 years of age (28 ± 8.1 years; $n = 29$) were recruited. There were 15 males of age 20–33 years (27 ± 3.8 years) and 14 females of age 20–46 years (27 ± 6.6 years). Subjects with past or present ocular diseases and diabetes were excluded. Subjects on contact lenses, with signs and symptoms of dry eye disease, or on topical medications were also excluded. Subjects using artificial tears were also excluded. Informed consent was obtained from all subjects before any measurements were undertaken. Most of the subjects were visitors or employees at the eye hospital (SankaraNethralaya, Chennai, India). The study protocol adhered to the tenets of the Declaration of Helsinki and approved by the Institutional Review Board at the eye hospital (Medical Research Foundation; Chennai, India).

Custom-made ocular spot fluorometer

A standard slit lamp was adapted to measure fluorescence from any desired spot in the anterior segment of the eye without axial scanning. An adjustable slit for the emitted light (referred to as the emission/collection slit) was placed confocal to the projection slit (a.k.a., the excitation/illumination slit) of the slit lamp to enable depth-resolved measurements. The size of the excitation slit was 4 mm x 0.5 mm for measurements in both the stroma and tear film. The emission slit was made equal to or slightly smaller than the excitation slit. For rejecting electronic noise as well as interference from the ambient light, we employed the principle of lock-in amplification for the detection of the emission. Accordingly, the excitation light intensity was modulated as a sine wave. This was achieved by replacing the halogen lamp of the slit-lamp with a high power white LED (10 Watts). The LED was modulated at 10 kHz using a custom-made LED driver (a linear amplifier with a bandwidth of 200 kHz), which was coupled to a standard function generator (Stanford Research Systems Inc., Model 345). The LED output was passed through a cobalt-blue filter to obtain the modulated excitation for fluorescein. Light through the emission/collection slit was passed through a barrier filter (530 ± 10 nm)

and then detected by a photomultiplier tube (PMT; R928HA; Hamamatsu, Inc). The output of the PMT and the sync output of the function generator were fed to the signal and reference inputs of a lock-in amplifier (Model 7260, Signal Recovery Inc., USA), respectively. The fluorescence measurements were recorded on the PC through a USB-GPIB interface at 100 Hz and were averaged further to minimize the noise. Specifically, the tear film and stromal fluorescence at each time point consisted of 15–20 samples taken over a period of 4 seconds. Each sample, in turn, was an average of more than 30–50 samples.

Epithelial permeability to fluorescein by the multi-drop method

We first provide an overview of the new multi-drop method and give details subsequently using Fig 1. First, a drop of low concentration fluorescein (referred to as the probe drop) is instilled, and the dynamics of its clearance from the ocular surface is measured using the fluorometer. Next, two loading drops containing a high concentration of fluorescein are instilled sequentially ~10 min apart, and the accumulation of the dye in the stroma is measured ~15 min after the second drop. These measurements along with the stromal thickness are then used to determine the corneal epithelial permeability to fluorescein (P_{dc}).

The concentration of fluorescein in the probe drop is small, and hence measurements of fluorescence from the tear film is devoid of concentration quenching. The driving force for the penetration of fluorescein into the stroma following the loading drops is estimated based on the dynamics of fluorescein clearance from the ocular surface for the probe drop. In other words, we assume that the fluorescein clearance of the loading drops from the ocular surface is equal to that of the probe drop. We use loading drops of high concentration to ensure higher accumulation of the dye in the stroma, which allows for measurements with a high signal-to-noise ratio (SNR). Since the accumulation of the dye in the stroma is usually very small even after the loading drops, the high concentration of the dye in the loading drops does not cause concentration quenching in the measurements of stromal fluorescence. Finally, based on the principles similar to those employed for the calculation of P_{dc} in the single-drop method, we have derived new equations to compute P_{dc} from measurements obtained with the multi-drop protocol.

Sodium fluorescein was obtained as a sterile 20% solution (Medimark Agencies, India). It did not contain benzalkonium chloride or other preservatives. Aliquots of topical drops were prepared quantitatively in sterile PBS as needed. All subjects underwent a general eye examination before experiments during which we recorded their central corneal thickness (CCT) by anterior segment OCT (SS-1000, Casia Tomey). Also, we measured autofluorescence from the corneal stroma. The fluorescence from the tears in the absence of fluorescein was negligible, and hence, autofluorescence from the tears was assumed zero. Subsequently, subjects underwent P_{dc} measurements as per the multi-drop protocol depicted by the timeline in Fig 1.

As per the protocol, we first instilled a 2- μ L drop of 0.35% fluorescein (probe drop) on the superior bulbar conjunctiva. The subjects were asked to blink a few times to ensure uniform spreading of the dye over the pre-corneal tear film. After 3–4 quick blinks, the clearance of fluorescein from the tears was measured by recording tear fluorescence every 15 seconds for the first 2 minutes and every 30 seconds after that until changes in the measured fluorescence became negligible. Subsequently, two 6 μ L drops of 2% fluorescein (loading drops) were administered 10 min apart. After 15 min of the second loading drop, the ocular surface and the fornices were washed using pre-formulated and sterile carboxymethyl cellulose (CMC) solution devoid of benzalkonium chloride or other preservatives. After the wash, fluorescence from the stroma was recorded 15–20 times and averaged to obtain the uncorrected

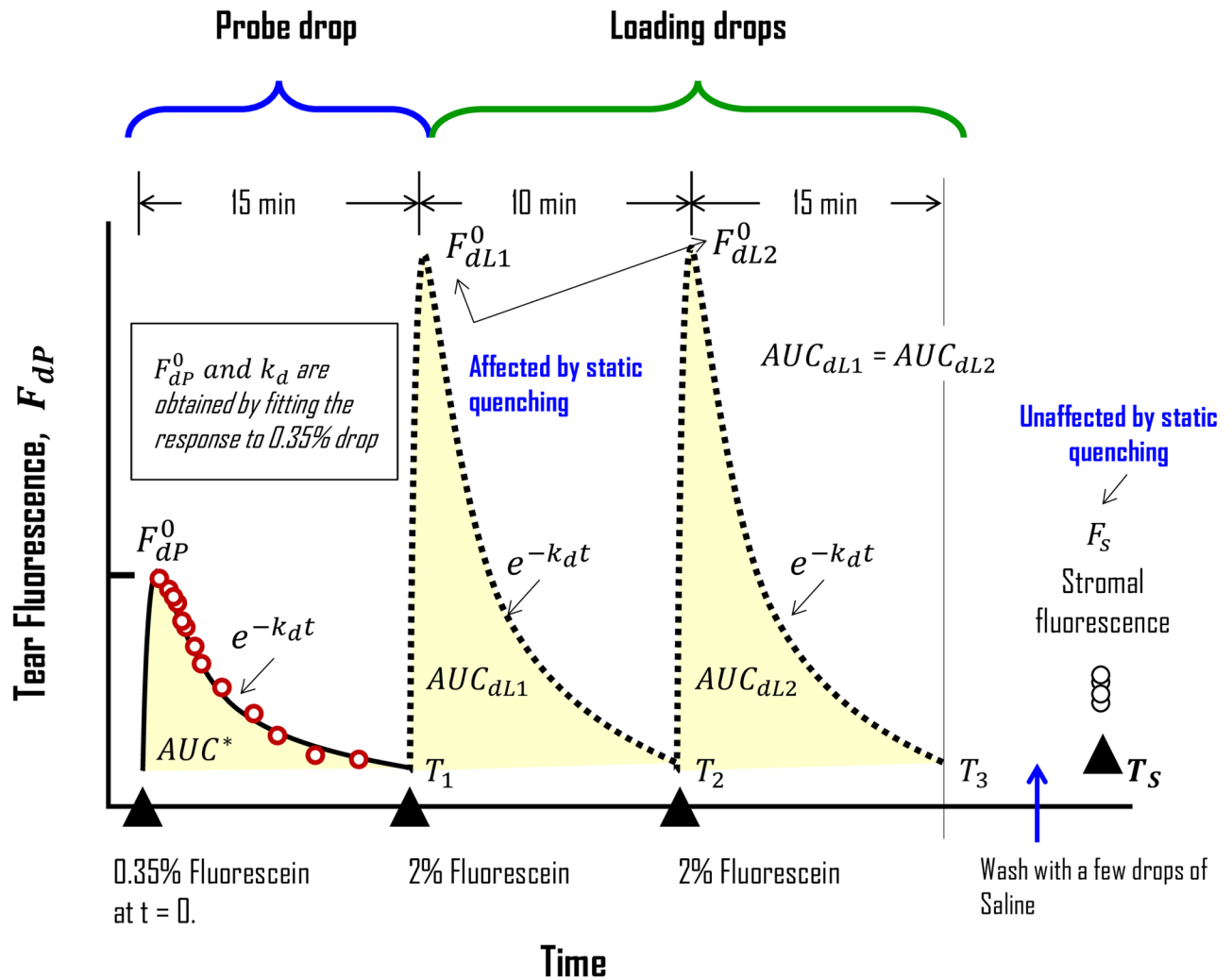


Fig 1. Schematic of the multi-drop protocol for the measurement of epithelial permeability. At $t = 0$, a 0.35% fluorescein drop (0.35 gm of fluorescein/100 mL PBS buffer) is instilled on the bulbar conjunctiva and the tear fluorescence is measured (shown by red unfilled circles). After clearance of the dye (usually < 15 min), two drops of 2% fluorescein (2 gm of fluorescein/100 mL PBS buffer) are instilled 10 min apart (T_1 and T_2). About fifteen minutes after the second drop, the ocular surface is washed with CMC solution (carboxymethyl cellulose solution; Blue arrow). Next, stromal fluorescence is measured 3–4 times at time T_s (usually within 5–10 min after T_3). AUC_{dl1} and AUC_{dl2} , which are assumed to be equal, are estimated based on the area under the curve calculated for the 0.35% drop (AUC^*). The tear fluorescence in response to the probe drop is fitted to a single-exponential decay to determine F_{dp}^0 and k_d . F_{dp}^0 is then used to estimate F_{dl1}^0 and F_{dl2}^0 . k_d for the 2% drops is assumed to be the same as that for the 0.35% drop. Hence, the first 0.35% drop is referred to as the probe drop. The 2% drops have been employed to load the stroma with measurable levels of fluorescein so that noise-free measurements of the stromal accumulation can be obtained. Therefore, the 2% drops are referred to as the loading drops.

<https://doi.org/10.1371/journal.pone.0198831.g001>

stromal fluorescence (uF_s). The corrected stromal fluorescence (F_s), which is indicative of accumulated fluorescein in the stroma, was obtained by subtracting the autofluorescence from uF_s . Although two loading drops were used, staining of the corneal epithelium was not noticed in any of the experiments (49 eyes of 29 subjects). This is consistent with the protocol employed for the measurement of corneal endothelial permeability wherein instillation of more than 7 drops of 5% fluorescein is typically employed [44, 64, 65].

Measured central corneal thickness (CCT), fluorescence clearance kinetics during the probe drop, and F_s were used to calculate P_{dc} as outlined below. All measurements for the estimated P_{dc} were performed by two examiners to avoid potential inter-observer variabilities.

Statistical analysis

The tear fluorescence curves were fitted to a single exponential decay by a non-linear least squares analysis using Prism 5.0 (GraphPad™ Software, Inc USA). The fitting to the decay was constrained to a steady state value of zero, consistent with autofluorescence of the tears being negligible. The comparison of the means of k_d for 2 and 6 μL drops in four different subjects was also performed with GraphPad™ based on Mann-Whitney U tests. The Monte Carlo Simulations (MCS) [66–68] (detailed in [S1 Appendix](#)), employed to evaluate the robustness of the experimental P_{dc} estimate, were carried out by a custom-made software program in LabVIEW (National Instruments Inc, Austin, TX).

Results

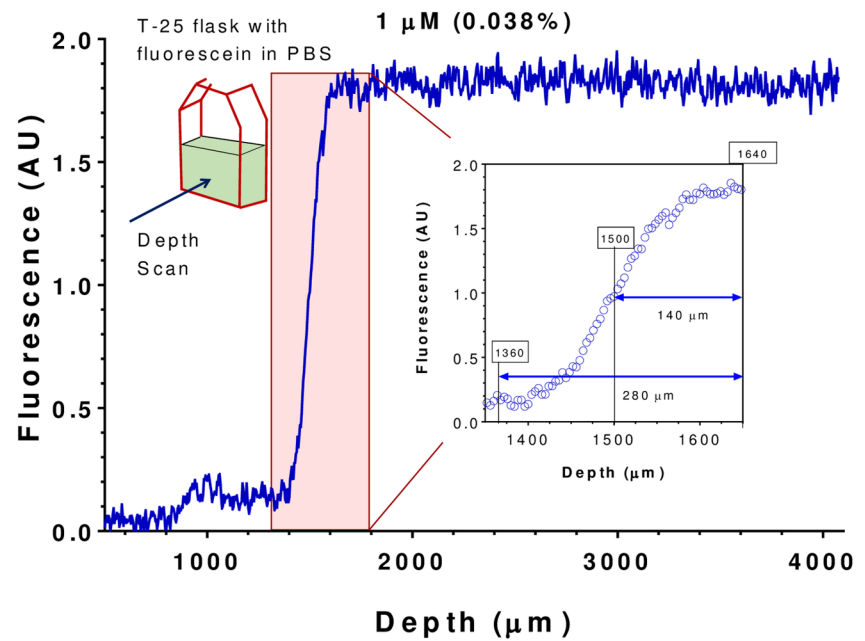
Linearity, sensitivity, and axial resolution of the spot fluorometer

We first assessed the linearity, sensitivity, and axial resolution of the custom-made spot fluorometer. These factors would be critical to assess the precision, reproducibility, and reliability of P_{dc} measurements. The investigations were carried out with fluorescein diluted in PBS at a pH of 7.4 contained in T-25 flasks. The flasks were held on a linear stage (coupled to a stepper motor) located at the chin rest of the fluorometer. Axial scans across the solution were performed under computer control (inset of [Fig 2A](#); Top Left). [Fig 2A](#) shows a typical fluorescence depth profile (blue line) with 1 μM fluorescein (i.e., 0.038% w/v of fluorescein). A steady level of fluorescence across the scanned depth shows the absence of concentration quenching. The measured fluorescence has a SNR (i.e., mean/SD of the signal) of 44, indicating a high measurement sensitivity. [Fig 2B](#) presents fluorescence vs. depth profiles at higher concentrations. At 50 μM (1.88% of fluorescein), a rapid decline in the measured fluorescence is observed with increasing depth. At 10 μM (0.38% fluorescein), a smaller decrease in the measured fluorescence with depth is noted. These findings suggest that concentration quenching occurs at concentrations $> 10 \mu\text{M}$. Based on these observations, we chose the concentration of the probe drop to be 0.35% for all our experiments. Thus, we ensured that none of our measurements is affected by non-linearity due to concentration quenching [29, 62].

The measurements in [Fig 2A](#) also highlight the depth resolution of the instrument. Specifically, the plot in the inset (unfilled circles; right side insert) indicates that the rise in fluorescence at the transition point from the flask into the fluorescein solution occurs over a depth of 280 μm (i.e., 1640 μm -1360 μm). In other words, the depth of the focal diamond formed by the intersection of the excitation and emission beams is $\sim 280 \mu\text{m}$. This axial resolution is better than what is known for Fluorotron Master™ ($> 0.5 \text{ mm}$) [56, 69, 70].

The potential impact of the depth of the focal diamond on the measured value of fluorescence in the stroma and tears is illustrated in [Fig 3](#). For measurements in tears, it is evident that the tear film does not span the depth of the focal diamond ([Fig 3B](#)). Moreover, since the stromal thickness is greater than the depth of the focal diamond, the measured fluorescence from the stroma is only proportional to the concentration of the dye in the stroma assuming that fluorescein does not bind to components of the stroma ([Fig 3C](#)). Since the tear film thickness (t_d) is smaller than the axial resolution of the instrument (δ), the ratio of the intersection volume of the focal diamond with the stroma to that with the tear film can be approximated by δ/t_d . We refer to this ratio as instrument correction factor or ICF ([Fig 3](#)). Assuming a tear film thickness of 3 μm [38, 41–43] and recalling $2\delta = 280 \mu\text{m}$, we assert that for our custom-made fluorometer, ICF is ~ 47 . For a given concentration of fluorescein, the fluorescence measured in the tear film should be multiplied by ICF to predict the fluorescence from the stroma at the same concentration.

A



B

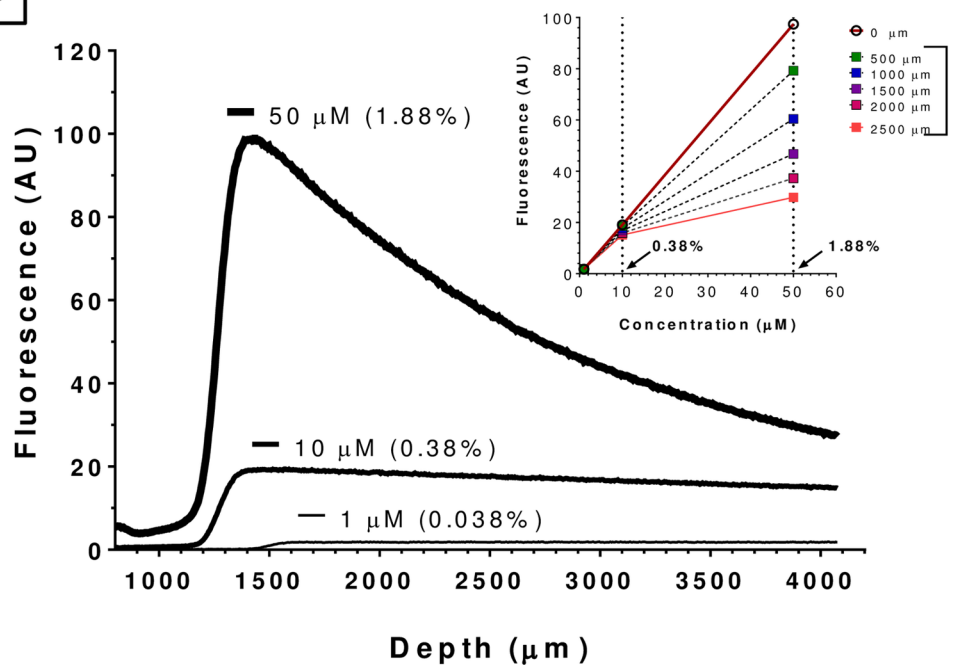


Fig 2. Linearity, depth resolution, and concentration quenching. Three solutions of fluorescein, prepared with PBS at 1, 10, and 50 μM (corresponding to 0.038%, 0.38%, and 1.88% (w/v), respectively) were contained in T-25 flasks. Depth-resolved fluorescence measurements were then obtained by positioning the flask along with the optical axis of the fluorometer. The angle between the excitation and the emission arms was held at 45° . Concentrations of fluorescein in % (provided in parenthesis) are in w/v basis. **Panel A:** Typical fluorescence vs. depth profile obtained with 1 μM solution. Note that the fluorescence of the solution remains constant over the depth of the scan. The

fluorescence change from background to the new plateau occurs over a transition depth $\sim 280 \mu\text{m}$ (inset on the right). This is a measure of the axial resolution of the instrument, which can also be specified as full-width at half maximum (FWHM; $140 \mu\text{m}$). **Panel B:** Fluorescence vs. depth profiles obtained with fluorescein at 1, 10, and $50 \mu\text{M}$ solutions. Unlike the fluorescence profile for $1 \mu\text{M}$ solution (thin line), the fluorescence for $50 \mu\text{M}$ (thick line) decreases with increasing depth, indicating concentration quenching. The fluorescence vs. depth profile for the $10 \mu\text{M}$ solution (0.38%) also shows concentration quenching, but it is marginal. Hence, the concentration of fluorescein in the probe drop was kept below 0.38% in all our experiments. The inset in Panel B summarizes the concentration quenching at different depths for the three different solutions.

<https://doi.org/10.1371/journal.pone.0198831.g002>

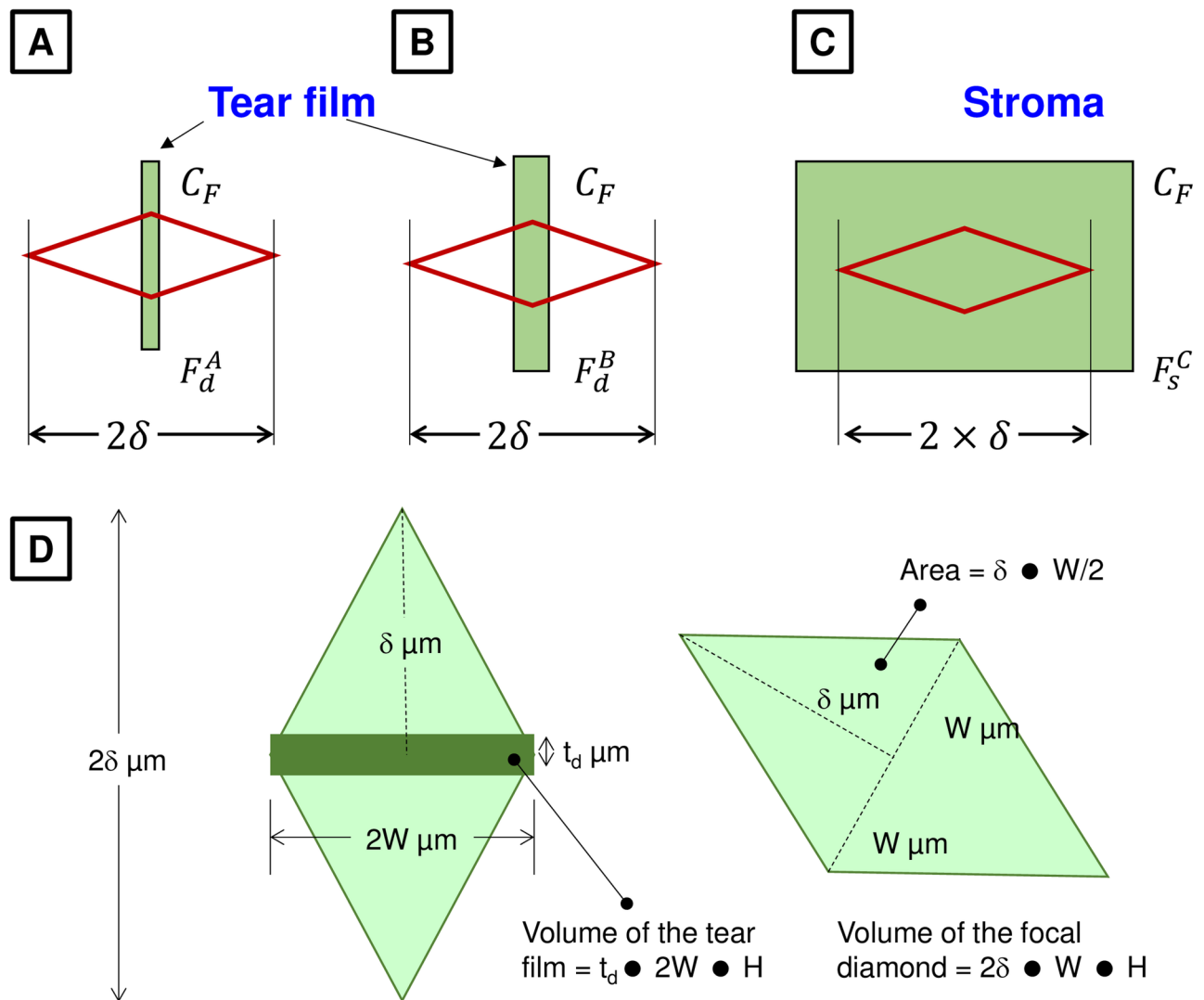


Fig 3. Effect of the axial resolution on the measured fluorescence. The depth of the focal diamond is 2δ . From Fig 2, we note that δ is $140 \mu\text{m}$. **Panel A:** Focal diamond (RED lines) across the tear film with fluorescein. Note that the tear film does not span the entire depth of the focal diamond. In the figure, F_d^A and C_F refer to the measured tear fluorescence and concentration of fluorescein in the tear film, respectively. **Panel B:** Tear film is thicker compared to that in Panel A so that $F_d^B > F_d^A$. **Panel C:** Focal diamond is positioned in the stroma. In this case, the measured fluorescence F_s^C would be proportional to C_F but independent of the stromal thickness, which is greater than 2δ . **Panel D:** Estimation of ICF. The intersection of the tear film with the focal diamond is a parallelepiped of volume given by $t_d \times 2W \times H$, where t_d is the thickness of the tear film, $2W$ is the maximum width of the focal diamond, and H is the thickness of the excitation slit beam. The volume of the focal diamond is given by $2\delta \times W \times H$, where 2δ is the axial resolution of the instrument ($2\delta \sim 280 \mu\text{m}$). Hence, the ratio of the volume of the focal diamond to that of volume of intersection between tear film and focal diamond (defined as ICF, instrument correction factor) is given by $(2\delta \times W \times H) / (t_d \times 2W \times H)$. Hence, ICF would be δ/t_d , which is equal to 47 assuming a tear film thickness of $\sim 3 \mu\text{m}$ [38, 41–43]. This estimation assumes that the fluorescence in the stroma for a given concentration of fluorescein is not different from an equivalent amount of fluorescein in water. More specifically, fluorescein is assumed unbound in the stroma.

<https://doi.org/10.1371/journal.pone.0198831.g003>

Dynamics of fluorescein clearance following the probe drop

For instilled drops of small volume V_i^0 , such as the probe drop (2 μL ; 0.35%), we assume the tear clearance of fluorescein to follow a single exponential decay [6, 71]. Therefore, the concentration of the dye in the tears at any time t (denoted by $C_{dp}(t)$) after instillation of the probe drop (Fig 1) can be written as

$$C_{dp}(t) = C_{dp}^0 e^{-k_d t} \tag{1}$$

Where C_{dp}^0 is the concentration of fluorescein in the tears at time $t = 0$. Table 3 below highlights all the mathematical notations.

C_{dp}^0 is dependent on the tear volume, instilled drop volume, and the concentration of fluorescein in the instilled drop. k_d is the elimination rate constant (with units of per min) which is influenced mainly by the blink frequency, tear secretion rate, tear outflow rate, tear evaporation, and the volume of tears.

Based on Eq 1, the half-life for fluorescein clearance can be given by $t_{1/2}^d = 0.693/k_d$ and is found to be 2–4 min in healthy eyes [44, 60]. Since the concentration in the instilled drop (0.35%) is less than the threshold for the onset of concentration quenching (< 0.38% as per Fig 2B), we assume a linear relationship between the concentration in the tears and the measured

Table 3. Mathematical notations.

Symbol	Description	Units
V_i	Instilled volume on the ocular surface	μL
C_{dp}	Concentration of the dye in the tears at any time t after the probe drop	μM
C_{dp}^0	Concentration of dye in the tears immediately ($t = 0$) after the probe drop	μM
k_d	Elimination rate constant	sec^{-1}
$t_{1/2}^d$	Half-life of the dye in tears = $0.693/k_d$	sec
F_{dp}	Tear fluorescence after the probe drop	mV
α	Proportionality constant for the calibration curve between tear fluorescence and concentration of the dye in the tears	$\mu\text{M}/\text{mV}$
F_{dp}^0	Tear fluorescence immediately ($t = 0$) after the probe drop	mV
AUC*	Area under the fluorescence curve following the probe drop	mV sec
P_{dc}	Corneal epithelial permeability to fluorescein	nm/sec
A	Surface area of the cornea	mm^2
m_s	Mass of fluorescein in the stroma	μg
Q	Mean stromal thickness	μm
C_{dl1}	Concentration of the dye in tears following loading drop 1	μM
C_s	Concentrations of the dye in the stroma	μM
F_s	Stromal fluorescence	mV
β	Proportionality constant for the calibration curve between tear fluorescence and concentration of the dye in the stroma	$\mu\text{M}/\text{mV}$
AUC _{dl1}	Area under the fluorescence curve following the first loading drop	mV sec
AUC _{dl2}	Area under the fluorescence curve following the second loading drop	mV sec
AUC _{dl}	$[\text{AUC}_{dl2}] = [\text{AUC}_{dl1}] = [\text{AUC}_{dl}]$	mV sec
M_p	Mass of the dye in the probe drop	μg
V_d	Volumes of tears	μL
M_L	Mass of the dye in the loading drop	μg
C_{dp}^0	Concentration of the dye in tears immediately following the probe drop	μM
C_{dl}^0	Concentration of the dye in tears immediately following the loading drop	μM
CCT	Central corneal thickness	μm

<https://doi.org/10.1371/journal.pone.0198831.t003>

tear fluorescence:

$$C_{dp}(t) = \alpha F_{dp} \tag{2}$$

Where α is the proportionality constant between tear fluorescence (F_{dp}) and fluorescein concentration ($C_{dp}(t)$). Applying Eq 2 at time $t = 0$,

$$C_{dp}^0 = \alpha F_{dp}^0 \tag{3}$$

As shown in Fig 3A, since the depth of the focal diamond is much larger than the thickness of the tear film, α would be dependent on the axial resolution of the instrument. Substituting Eqs 2 and 3 in Eq 1, we get

$$F_{dp}(t) = F_{dp}^0 e^{-k_d t} \tag{4}$$

Integrating both sides of Eq 4 with respect to time (between 0 and time T), we get

$$[AUC_p] = F_{dp}^0 \int_0^T e^{-k_d t} dt = \frac{F_{dp}^0}{k_d} (1 - e^{-k_d T}) \tag{5}$$

where $[AUC_p] = \int_0^T F_{dp} dt$ is the area under the tear fluorescence curve following the probe drop.

For large T ($5 \times t_{1/2}^d$ or i.e., >10 min), Eq 5 above simplifies to

$$[AUC_p] = \frac{F_{dp}^0}{k_d} \tag{6}$$

As mentioned earlier, concentration quenching is not observed at 0.35% of fluorescein (Fig 2B) [29, 62]. Therefore, the probe drop allows for the estimation of k_d and F_{dp}^0 in Eq 6 without any influence of concentration quenching. Both parameters can be estimated by fitting Eq 1 to tear fluorescence vs. time data after the probe drop. Fig 4 shows the variability of the tear fluorescence dynamics between subjects. The repeatability in a given subject of the tear-fluorescence decay profiles is presented in Fig 5.

Fluorescein accumulation in the stroma after the loading drops

The loading drops contain 2% fluorescein (Fig 1). Therefore, accumulation of fluorescein in the stroma would be significant when compared to the accumulation following probe drop, which was negligible in our experiments. Increased accumulation will allow us to precisely measure the stromal fluorescence, and hence accurately estimate P_{dc} . In the following, we relate P_{dc} quantitatively to the accumulation of fluorescein in the stroma in response to the two loading drops. First, we define corneal epithelial permeability to fluorescein (P_{dc}) by the following phenomenological equation:

$$\frac{dm_s}{dt} \stackrel{\text{def}}{=} P_{dc} A (C_{dl1} - C_s), \text{ where } m_s = Q A C_s \tag{7}$$

In Eq 7, m_s is the mass of fluorescein in the stroma, A is the surface area of the cornea, and Q is the mean stromal thickness. ($Q \times A$) is the stromal volume. C_s and C_d refer to concentrations of fluorescein in the stroma and tears, respectively. Specifically, C_{dl1} is the concentration of fluorescein in the tears following the first loading drop. Substituting for m_s and assuming

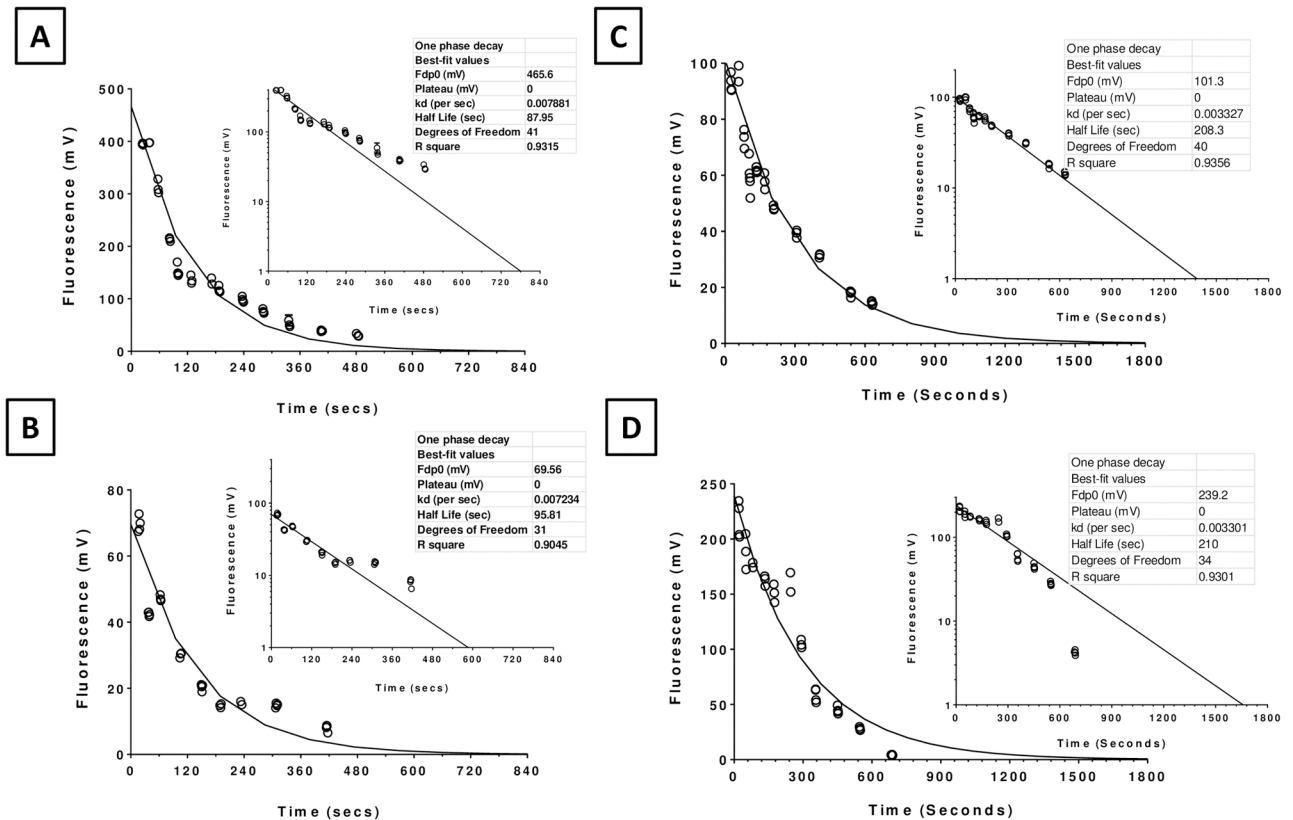


Fig 4. Inter-subject variability of fluorescein clearance after the probe drop in two subjects. The excitation slit was focused on the tear film and the fluorescence vs. time profile was obtained for 10 min. F_{dp}^0 and k_d are the intercept and slope, respectively, of the fluorescence decay in the tear film as per the exponential decay curve (Eq 4) using non-linear least squares. Half-lives $t_{1/2}^d$ indicated in the inset were calculated from k_d . **Panels A and B:** Data from a subject showing rapid clearance of fluorescein with half-lives of only 88 and 96 seconds in the left and right eyes, respectively. **Panels C and D:** Data from a different subject showing a relatively slower clearance with half-lives of 208 and 210 seconds in the left and right eyes, respectively.

<https://doi.org/10.1371/journal.pone.0198831.g004>

$C_S \ll C_{dL1}$ at all times, we can rewrite Eq 7 as

$$Q \frac{dC_s}{dt} = P_{dc} C_{dL1} \tag{8}$$

Since the accumulated fluorescein in the stroma is within the limits of concentration quenching ($\ll 0.35\%$ fluorescein; measured stromal concentration following the loading drop 1), we again assume linearity between measured F_s and the stromal concentration C_s . Thus,

$$C_s(t) = \beta F_s \tag{9}$$

Where β is the proportionality constant between the measured stromal fluorescence F_s and the concentration of fluorescein in the stroma ($C_s(t)$).

Applying Eqs 2 and 9, we can rewrite Eq 8 as

$$\beta Q \frac{dF_s}{dt} = P_{dc} \alpha F_{dL1} \tag{10}$$

We note that the calibration constants α and β are not identical because the depth of the focal diamond is larger than tear film ($\sim 3 \mu\text{m}$) but smaller than the stromal thickness ($\sim 480 \mu\text{m}$; Fig 3).

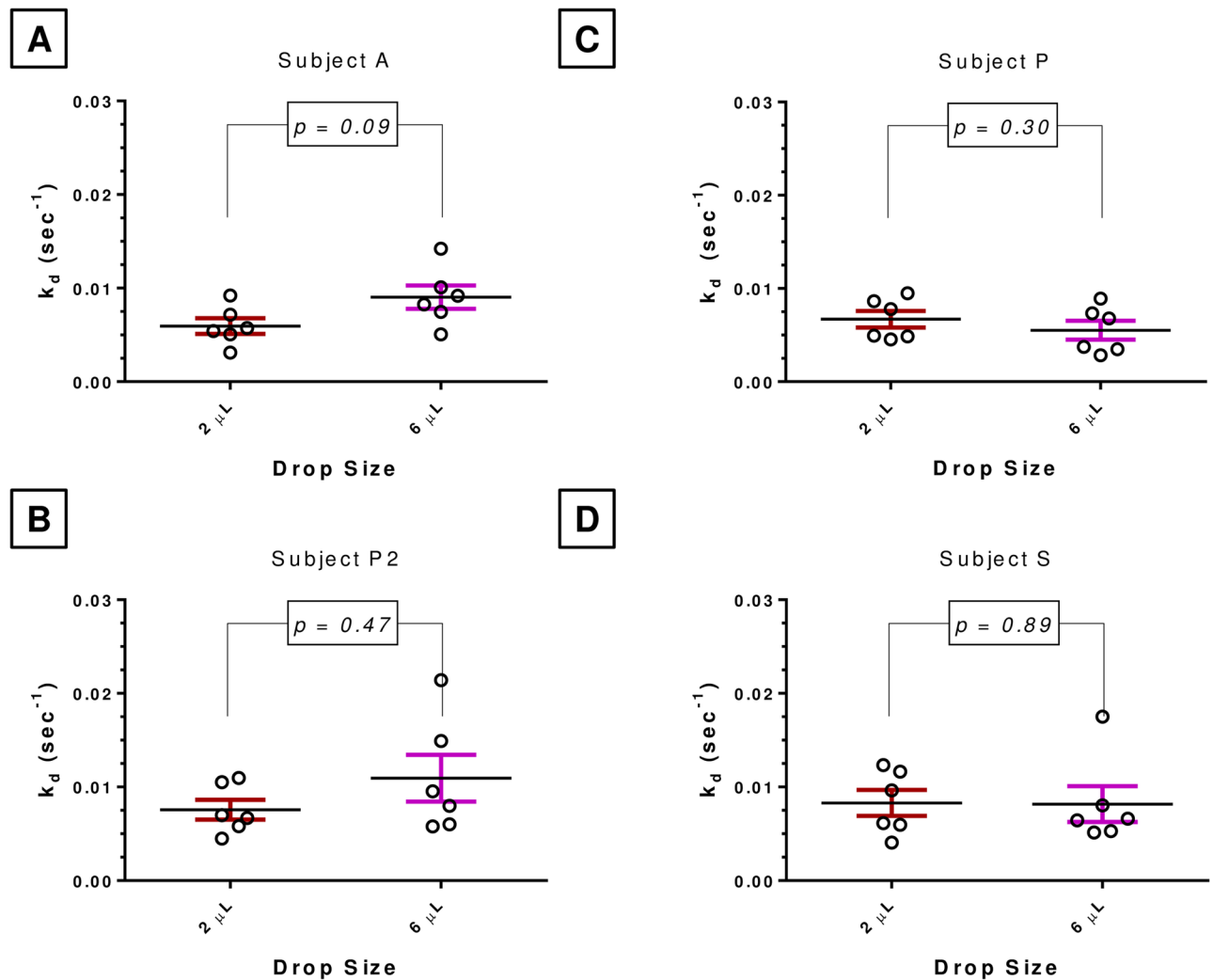


Fig 5. Effect of instilled volume on fluorescein clearance (k_d) in four different subjects. The data also shows the intra-subject variability of fluorescein clearance in repeat trials. **Panels A-D** show k_d estimated from independent probe drops of fluorescein (0.35%) at 2 or 6 μL each dropped in a single subject ~ 15 min apart. Paired t-tests show lack of any significant difference between the means of k_d measured at the two instilled volumes.

<https://doi.org/10.1371/journal.pone.0198831.g005>

Integrating both sides of Eq 10 with respect to time between T_1 and T_2 (as specified in Fig 1), we get

$$\beta Q [F_s(T_2) - F_s(T_1)] = P_{dc} \alpha [AUC_{dl1}] \quad (11)$$

where $[AUC_{dl1}] = \int_{T_1}^{T_2} F_{dl1} dt$ is the area under the fluorescence curve following the first loading drop.

Since we administer another drop at T_2 (Fig 1), similar to Eq 11, we can write

$$\beta Q [F_s(T_3) - F_s(T_2)] = P_{dc} \alpha [AUC_{dl2}] \quad (12)$$

where $[AUC_{dl2}] = \int_{T_2}^{T_3} F_{dl2} dt$ is the area under the fluorescence curve following the second loading drop.

Adding Eqs 11 and 12, we get

$$\beta Q[F_s(T_2) - F_s(T_1) + F_s(T_3) - F_s(T_2)] = P_{dc} \alpha ([AUC_{dl1}] + [AUC_{dl2}]) \quad (13)$$

Since the two loading drops are identical at T_1 and T_2 (volumes and location on the bulbar conjunctiva), as a first approximation, we claim

$$[AUC_{dl2}] = [AUC_{dl1}] = [AUC_{dl}]$$

This simplifies Eq 13 to

$$\beta Q[-F_s(T_1) + F_s(T_3)] = 2 P_{dc} \alpha [AUC_{dl}] \quad (14)$$

Since fluorescein in the stroma before the first loading drop at T_1 is negligibly small ($F_s(T_1) \sim 0$), Eq 14 implies that

$$P_{dc} = \frac{Q \beta F_s(T_3)}{2 \alpha [AUC_{dl}]} \quad (15)$$

where $F_s(T_3)$ is the average stromal fluorescence measured ~ 15 min after instillation of the second drop (i.e., at T_s in Fig 1). In general, α is the proportionality constant for F_d vs. C_d so that $C_d = \alpha \times F_d$. Also, β is the proportionality constant for F_s vs. C_s so that $C_s = \alpha \times F_s$. Since the tear film thickness is less than that of the focal diamond, $\alpha < \beta$. We also note that Eq 15 is valid for small T_3 (< 30 min) so that the loss of fluorescein from stroma across the endothelium remains negligible.

Calculation of the epithelial permeability

As per Eq 15, we need to know $Q, \alpha, \beta, F_s(T_3)$ and $[AUC_{dl}]$ for calculating P_{dc} after instillation of two loading drops of 2% fluorescein. The value of $[AUC_{dl}]$ can be estimated based on the dynamics of fluorescein clearance of the probe drop. We estimate from the probe drop because any tear fluorescence measurements after the loading drops (2% fluorescein) would be confounded by concentration quenching, for which the threshold is 0.38% (Fig 2). For the estimation of $[AUC_{dl}]$, we define V_i and V_d as the volumes of the instilled drop and the tears, respectively. Further, we define M_p as the mass of fluorescein in the probe drop. Then, we can write the following equation to determine the concentration of fluorescein immediately after the instillation of the probe drop and subsequent mixing with the tears:

$$C_{dp}^0 = \frac{M_p}{V_i + V_d} \quad (16)$$

This equation assumes no spillover of the tears following the probe drop (2 μ L) and complete mixing. Similarly, if M_L denotes the mass of fluorescein in the loading drops (6 μ L), we can write the following equation for the concentration of fluorescein immediately after the instillation of the loading drops and their complete mixing in the tears:

$$C_{dl}^0 = \frac{M_L}{V_i + V_d} \quad (17)$$

Assuming $C_{dp}^0 = \alpha F_{dp}^0$, fluorescence from the 2 μ L probe drop at time $t = 0$ can be written from Eq 16 as

$$F_{dp}^0 = \frac{M_p}{\alpha (2 + V_d)} \tag{18}$$

where F_{dp}^0 represents the tear fluorescence at $t = 0$ following the probe drop.

Similarly, for 6- μ L loading drops, fluorescence at time $t = 0$ can be written from Eq 17 as

$$F_{dl}^0 = \frac{M_L}{\alpha (6 + V_d)} \tag{19}$$

Dividing Eq 19 by 18, we get

$$\frac{F_{dl}^0}{F_{dp}^0} = \frac{M_L (2 + V_d)}{M_p (6 + V_d)} \tag{20}$$

Now, similar to Eq 6, we can calculate $[AUC_{dl}]$ as

$$[AUC_{dl}] = \frac{F_{dl}^0}{k_d}$$

Substituting for F_{dl}^0 in Eq 20, we get

$$[AUC_{dl}] = F_{dp}^0 \frac{1}{k_d} \frac{M_L (2 + V_d)}{M_p (6 + V_d)} \tag{21}$$

In other words, $[AUC_{dl}]$ necessary for calculating P_{dc} can be obtained from F_{dp}^0 and k_d , which are determined by the instillation of the probe drop. Hence, for the two-drop protocol, we calculate P_{dc} based on Eqs 15 and 21 by

$$P_{dc} = \frac{k_d Q \beta F_s(T_3) M_p (6 + V_d)}{2 \alpha F_{dp}^0 M_L (2 + V_d)} \tag{22}$$

Thus, assuming a value for V_d , we can calculate P_{dc} knowing $Q, \alpha, \beta, F_s(T_3), k_d$ and F_{dp}^0 . M_p and M_L are fixed at 0.35% and 2% for probe and loading drops, respectively. The mean stromal thickness (Q) was calculated as $[(1.06 \times CCT) - 50]$, where CCT is the central corneal thickness as measured by OCT in our experiments. We have assumed epithelial thickness to be 50 μ m on average. The formula for the average stromal thickness was obtained from 68 eyes in independent experiments based on OCT measurements. Referring to Eqs 3 and 9, we also note that β/α in Eq 22 is equal to ICF (~ 47 for our instrument).

Measurement of permeability

As shown in the timeline for the protocol (Fig 1), our first step was to assess dynamics of fluorescein clearance in a given subject by a probe drop. The data was then used to estimate k_d and F_{dp}^0 in order to calculate P_{dc} by Eq 22. As noted before, Fig 4 shows the typical profiles of fluorescence decay following the probe drop. The estimation of F_{dp}^0 and the curve fit to tear fluorescence data requires measurement of tear fluorescence immediately after the administration of the probe drop. In most subjects, the first measurement could be made in less than ~ 20 seconds after administering the probe drop. The tear fluorescence data invariably showed single exponential decay kinetics as expected. These could be fitted to Eq 1 with the correlation coefficient typically > 0.9 . Since the tear fluorescence before the probe drop is negligible, the fitting

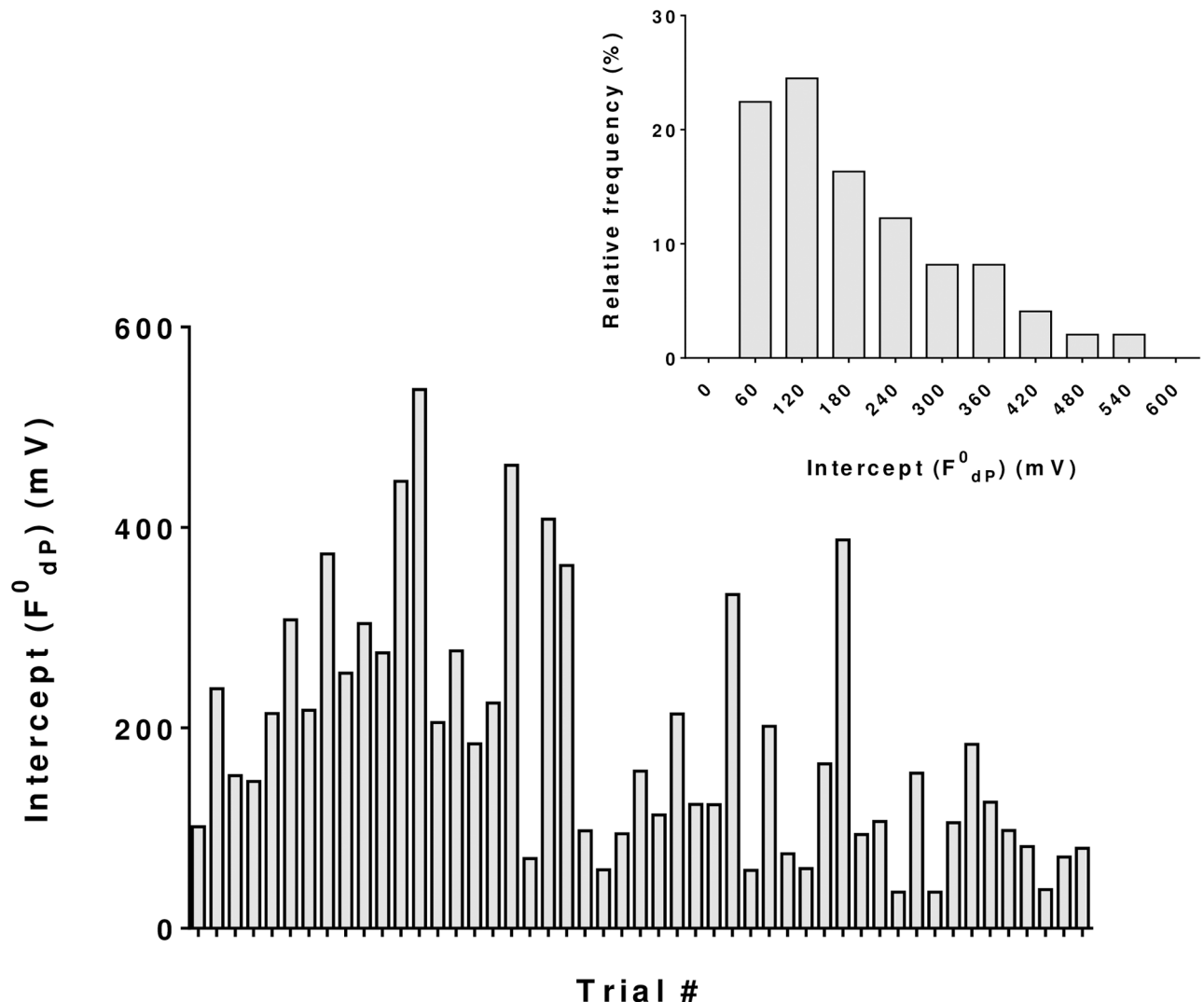


Fig 6. Estimated tear fluorescence at time $t = 0$ after instillation of the probe drop (F^0_{dp}). The Y intercept (tear fluorescence at $t = 0$, F^0_{dp}) of the fluorescence vs. time plot was obtained by fitting data to the exponential decay as per Eq 4: $\ln F_{dp}(t) = \ln F^0_{dp} - k_d t$. The mean and SD values are 206.51 and 113.89 mV, respectively ($n = 49$ eyes and 29 subjects).

<https://doi.org/10.1371/journal.pone.0198831.g006>

of tear fluorescence vs. time to single exponential decay kinetics was constrained to a steady state value of zero.

The fluorescence at time $t = 0$ (F^0_{dp}) which is dependent on the tear volume, varied by ~ 9-fold (206 ± 113.9 ; 49 eyes of 29 subjects), as depicted in Fig 6. Similarly, in agreement with variations in the tear flow rate, blink frequency, and tear volume, k_d varied from 0.0015 sec^{-1} to 0.044 sec^{-1} ($0.014 \pm 0.010 \text{ sec}^{-1}$; 49 eyes of 29 subjects) (Fig 7). This corresponds to a variation in the half-life from 53 seconds to 210 seconds (Fig 4).

At 15 minutes following the probe drop, the stromal fluorescence (F_s (T1)) did not increase significantly beyond the baseline ($p < 0.05$). However, after the two loading drops, F_s (T3) (denoted as F_s (Ts)) increased by 10-fold compared to the background ($p < 0.05$; 10.19 ± 8.22). Moreover, F_s could be measured accurately (with a SNR > 44). Also, F_s (Ts) did not exceed the fluorescence corresponding to 0.38% fluorescein. Hence, F_s (Ts) measurements are also not confounded by concentration quenching.

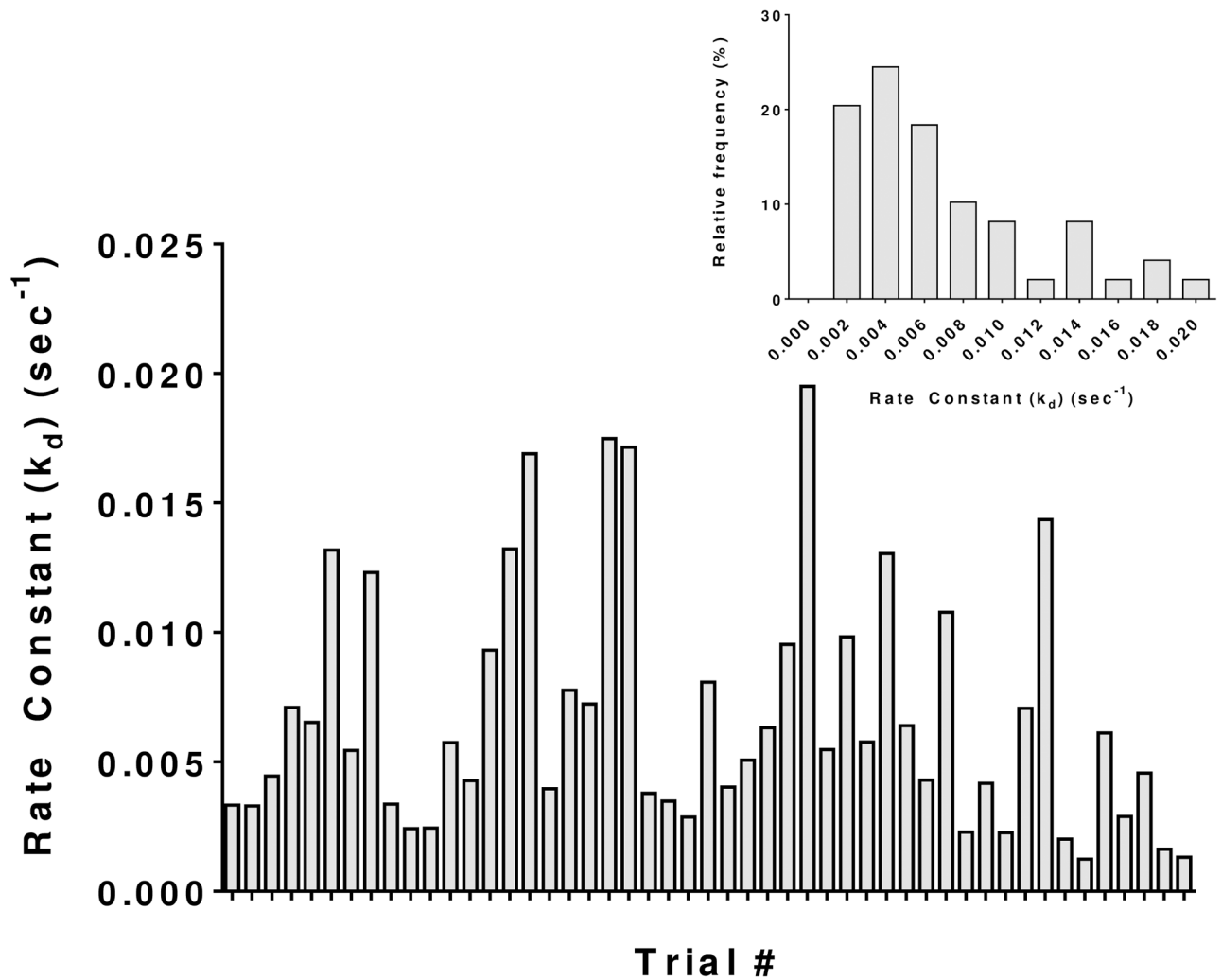


Fig 7. Estimated fluorescein elimination rate constant (k_d) following instillation of the probe drop. k_d was obtained as the slope of the fluorescence decay by fitting to Eq 4 according to $\ln F_{dp}(t) = \ln F_{dp}^0 - k_d t$. The mean and SD values are 0.0142 and 0.0107 sec^{-1} , respectively ($n = 49$ eyes and 29 subjects).

<https://doi.org/10.1371/journal.pone.0198831.g007>

Finally, we calculated P_{dc} for each eye by Eq 22 using estimated k_d and F_{dp}^0 values along with measured $F_s(T_s)$ and Q (Raw data of all subjects is provided in S1 File). The calculated P_{dc} was 0.54 ± 0.54 nm/sec and its distribution is given by the histogram shown in Fig 8. The inset shows the histogram of P_{dc} for 49 eyes of 29 subjects. The median of P_{dc} was 0.32 nm/sec (0.07 nm/sec to 2.59 nm/sec). These calculations have been further examined by Monte Carlo simulation (i.e., MCS) [66–68] to ‘expand’ the sample size of our study and investigate the impact of the model and parameter uncertainties on the estimated P_{dc} . The details are given in the S1 Appendix.

Discussion

As a hydrophilic dye [39, 41, 72], fluorescein penetrates the corneal epithelium mainly via the paracellular pathways. Hence, changes in P_{dc} indicate either apoptosis or disruption of tight junctions. Thus, an accurate measurement of P_{dc} is of paramount importance in characterizing subtle changes in the health of the ocular surface. In addition, fluorescein is frequently

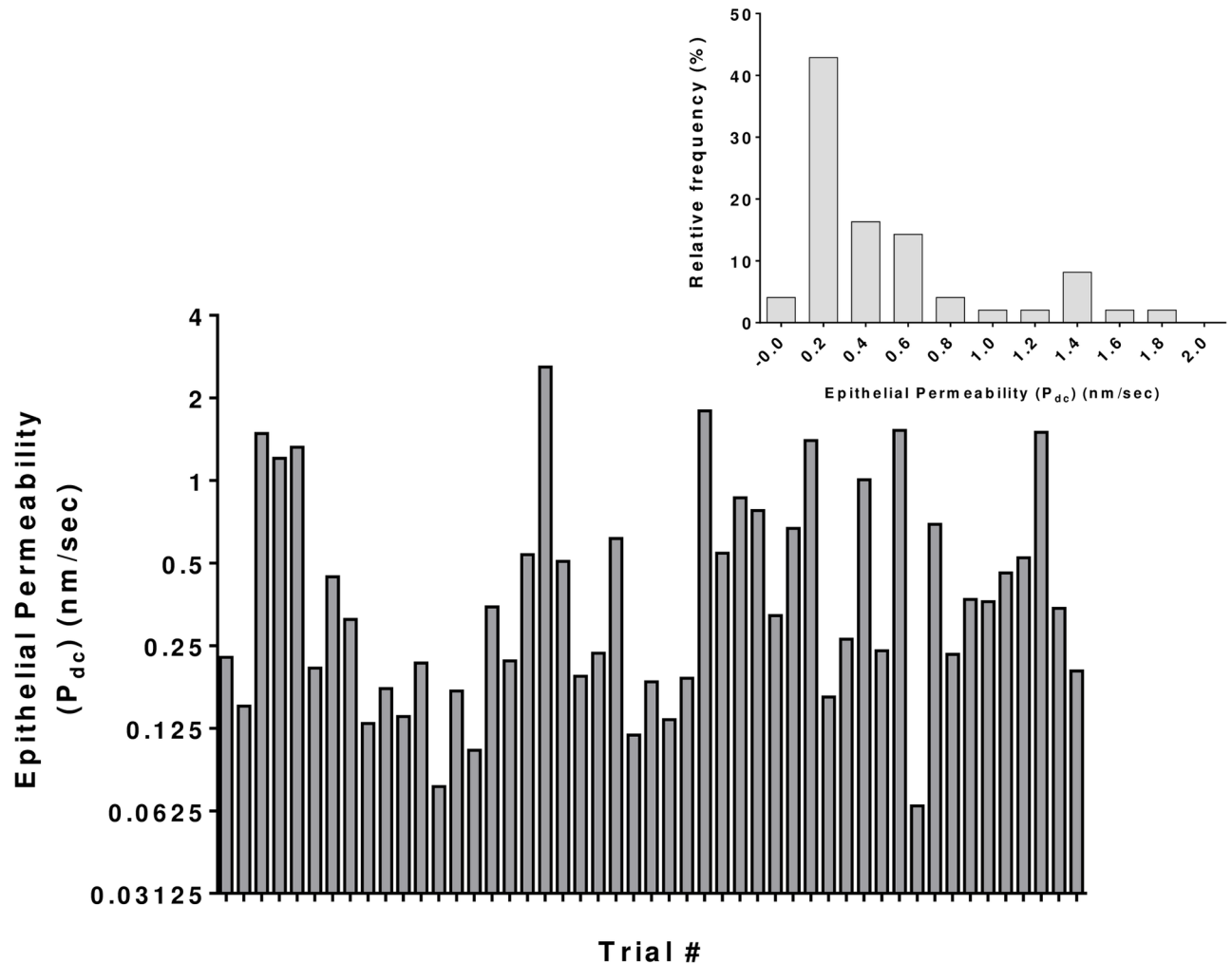


Fig 8. Calculated permeability of the corneal epithelium in healthy subjects. The values of P_{dc} (as calculated by Eq 22) ranged from 0.07 nm/sec to 2.59 nm/sec. The mean and SD are 0.54 and 0.54 nm/sec, respectively ($n = 49$ eyes and 29 subjects; median = 0.32 nm/sec).

<https://doi.org/10.1371/journal.pone.0198831.g008>

employed as a fluorescent drug analog to probe the kinetics of topical ocular drug delivery [41, 71, 73, 74]. Based on these rationale, we developed a novel spot fluorometer and established a multi-drop method to reassess P_{dc} in a clinical setting.

Unlike the commonly employed commercial ocular fluorometer (i.e., Fluorotron Master™, Ocumetrics Inc. Palo Alto, CA), our spot fluorometer does not perform axial scans across the depth of the anterior segment. Instead, it enables measurements from any spot on the ocular surface or within the eye. As a starting point, in order to assess both the new protocol and the new spot fluorometer, we focused on measurements of P_{dc} in a cohort of healthy subjects. We have found the value of P_{dc} to be 11-fold higher than the values reported using the single-drop method [29, 37]. Although our data does not provide reasons for the observed discrepancy between estimated values by the two methods, we note that the current estimates based on the multi-drop method is closer to values reported for drugs with an octanol-water partition coefficient and molecular weight equivalent to that of fluorescein [57] (Tables 1 and 2).

Measurements in the multi-drop method are devoid of concentration quenching

While designing the multi-drop protocol, attention was paid to two general problems of ocular fluorometry: (a) loss of fluorescence sensitivity with an increase in axial resolution of the instrument and (b) concentration quenching [29, 37]. With the excitation and emission slit widths at $\sim 140 \mu\text{m}$ and the angle between excitation and emission arms at 45° , we found the axial resolution of our new spot fluorometer to be $\sim 280 \mu\text{m}$ (Fig 2). Concentration quenching, which is dependent on the concentration of fluorescein [61], began to manifest at concentrations exceeding 0.38% for the combination of instrument settings that we employed in our measurements (Fig 2B). In experiments with Fluorotron Master™, others have indicated that fluorescein $> 0.35\%$ results in concentration quenching [29, 36]. Therefore, with fluorescein restricted to 0.35%, our measurements of tear fluorescence after the probe drop are devoid of nonlinearity. In other words, the estimated k_d and F^0_{dp} are not confounded by concentration quenching. In contrast to the probe drop, the loading drops contained 2% fluorescein (Fig 1), which can readily cause concentration quenching (inset in Fig 2A). Therefore, we did not measure fluorescein clearance after administering the loading drops (Fig 1). In other words, k_d and F^0_{dl} (shown as F^0_{dl1} and F^0_{dl2} in Fig 1) were not measured based on the clearance of fluorescein following the loading drops. F^0_{dl} , in particular, was obtained by scaling F^0_{dp} (Fig 1). k_d is assumed to be the same between the probe and the loading drops, as confirmed in Fig 5.

Our goal for the use of the loading drops, therefore, was to secure an enhanced accumulation of fluorescein in the stroma so that stromal fluorescein levels could be measured with high SNR. As expected, the two loading drops at 2% and 6 μL led to sufficiently high F_s , and its measurements could be performed at a high SNR of 44. Alternatively, we note that the observed standard error in the measurement of F_s was $< 3\%$. Overall, the measurements of stromal fluorescence are arguably more accurate in the multi-drop protocol. Hence, the multi-drop method has the potential to yield a more precise measurement of P_{dc} . Moreover, Eq 15 for the calculation of P_{dc} can easily be extended to any number of loading drops. Specifically, we can rewrite Eq 15 for “n” number of loading drops as follows:

$$P_{dc} = \frac{Q \beta F_s(T_{n+1})}{n \alpha [AUC_{dl}]} \quad (23)$$

where $F_s(T_{n+1})$ is the average stromal fluorescence measured ~ 15 min after administration of the n^{th} drop. Increasing the number of loading drops, however, results in an increase in the overall time taken to perform P_{dc} measurements. Compared to the single-drop method, the time taken for two loading drops involves an additional 20–30 min to the protocol (Fig 1). Apart from this drawback, no other methodological problems are apparent in the new multi-drop protocol. None of the subjects showed any adverse reactions, including epithelial staining, in response to two loading drops. In hindsight, it appears that the measurement period for the probe-drop and time between the loading drops can be further compressed to reduce the overall duration of the multi-drop method. Further reduction in the duration of the protocol is also appropriate to limit the loss of fluorescein into the anterior chamber, which is negligibly small in our calculations.

Corneal epithelial permeability is higher than previously reported

In contrast to several earlier reports based on the single-drop method and the bath technique [28, 30, 32, 35–37, 75–78], we have found mean P_{dc} to be at least 11-fold higher (Table 1). The average age of the subjects for the single-drop studies by McNamara et al. [37] was ~ 30 years, which is comparable to 28 ± 8.1 years in the current study. Thus, with age difference between

the subjects in the two studies kept to a minimum, the difference in the reported values of P_{dc} is noteworthy. Our estimate of P_{dc} , however, is closer to the permeability of many drugs across the corneal epithelium, especially those with molecular weights and octanol-water partition coefficients close to that of fluorescein [57–59] (Table 2). Moreover, permeability estimates based on computed partition coefficients [79] are also closer to the range of P_{dc} reported in this study. Although the discrepancy is significant, we have not been able to ascertain the cause with certainty. Additional studies in the future will unravel the definitive cause. However, the following points can be made regarding the two methods. The single-drop method results in low levels of stromal accumulation of fluorescein and hence is likely to show high variability in the measurements. In the proposed multi-drop method, the stromal accumulation is enhanced significantly relative to the single-drop method. Since the spot fluorometer is of high axial resolution (i.e., smaller focal volume), the stromal fluorescence is less likely to be confounded by levels of fluorescein in the aqueous humor. Overall, the high axial resolution in the current study and the potential for higher SNR in the stromal measurements tend to suggest that the data obtained in this study are accurate. Based on these observations, we believe that the reported value of P_{dc} could be impacted by a combination of factors including the protocol and characteristics of the instrument.

Variability in the measured corneal epithelial permeability

Despite improvements in reducing the measurement errors, the variability in the measured P_{dc} is high, with a standard error of 0.078 ($n = 49$ eyes of 29 subjects). This could be mainly due to a high variability in the dynamics of fluorescein clearance (Figs 4, 6 and 7), which is affected by tear secretion, blink rate, lacrimal drainage, tear evaporation rate, and tear volume. In this context, we note that the bath technique maintains a steady concentration gradient for transport across the epithelium, and hence can avoid problems due to variability in fluorescein clearance. However, the bath technique is not suitable, as washing off fluorescein from the ocular surface and its adnexa is cumbersome and can be incomplete, leading to errors in the measurement of F_s (Ts).

Our initial attempts to measure P_{dc} by the single-drop method were unsuccessful because accurate measurements of F_s (Ts) could not be made with our spot fluorometer. As noted earlier, the relatively higher axial resolution of our instrument may have led to a reduction in sensitivity. However, 0.35% probe drop led to sufficiently high levels of the dye in the tears for an accurate assessment of k_d and F_{dp}^0 (Figs 4–6). Moreover, since the lock-in amplifier rejects external light, we also note that the tear fluorescence measurements were not confounded by fluctuations in the ambient light. In addition, the passage of any reflected excitation light to the photomultiplier is negligible because of the confocal optics of the spot fluorometer. This is evident in the autofluorescence values in our measurements. Thus, we conclude that the physiological variations in tear dynamics contribute to the observed variability in k_d and F_{dp}^0 . Instrumental and observer errors are relatively small. Furthermore, to establish the robustness of our experimental P_{dc} estimate, we undertook MCS (S1 Appendix). After 10,000 iterations, as shown in Fig A1, MCS produced an estimate of P_{dc} close to that of the experimental value. If our assumptions in the derivation of Eq 22 were to be incorrect or if our experimental measurements erroneous, the MCS estimate of P_{dc} would have been significantly different from the experimental P_{dc} .

Practical implications

In addition to the clinical applications of P_{dc} as a marker of corneal epithelial health, its accurate measurement is critical for modeling drug transport across the cornea. As a hydrophilic

tracer, fluorescein is commonly employed as a drug analog in evaluating drug delivery vehicles including gels and polymeric implants [71, 74]. In these situations, the necessary pharmacokinetic models could use an accurate estimate of P_{dc} .

Conclusions

In summary, we have developed a new protocol for measuring the permeability of fluorescein across the corneal epithelium using our custom-made spot fluorometer. The new fluorometer has an axial resolution of 280 μm , which is better than the resolution noted with other fluorometers [7, 12]. The measurement protocol, especially suitable for experiments with human subjects, is simple and involves a probe drop followed by two loading drops administered sequentially. In a cohort of 29 subjects (49 eyes), we have found P_{dc} to be 0.54 nm/sec. This value is 11-fold higher than the previous reports for fluorescein. However, it is close to the permeability of a wide variety of drugs with similar partition coefficients and molecular weights [58].

Supporting information

S1 Appendix. Monte Carlo simulations.

(DOCX)

S1 Fig. Summary of the Monte Carlo simulations. Panels A-E show distribution profiles of various parameters that produced a P_{dc} histogram similar to those of the measured values shown in the inset of Fig 8. Initially, we assumed parameters to follow either normal or Weibull distribution. Specifically, the parameters k_d , F_{dp}^0 , and F_s (Ts) were assumed to follow Weibull distribution in order to obtain a positively skewed distribution for P_{dc} similar to that observed in our experimental findings (inset of Fig 8).

(TIF)

S1 File. Raw data of experiments with human subjects for epithelial permeability. Identification of the subjects has been masked with numbers. The data is provided as follows: Column A: Subject ID (masked), Column B: Sex (M: Male; F: Female), Column C: Age—rounded off (in years), Column D: 1 refers to Right Eye and 2 refers to Left Eye, Column E: CCT (μm)—Central corneal thickness in micrometers as measured using OCT (Casia SS 1000), Column F: Q nm—Stromal thickness, expressed in nm, Column G: k_d (per sec)—Slope; obtained by fitting decay curve of the probe drop, Column H: fdp_0 —Same as F_{dp}^0 , obtained by fitting decay curve of the probe drop, Column I: F_{ds} —Stromal fluorescence after 2 loading drops, Column J: F_{ds} —Correction application for changes in slit width and PMT gain, Column K: ratio—Correction factor for drop size and concentration of fluorescein in the loading drop, Column L: P_{dc} —In nm/sec, calculated as per Eq 22 in the main text but without instrument correction factor (i.e., ICF = 47), and Column M: P_{dc} : In nm/sec, calculated as per Eq 22 in the main text.

(XLSX)

Acknowledgments

We thank all the participants of the study. We also thank Subashree Murugan, Kaveet Pandya, and Kushal Shah for help in preparing the revisions to the original manuscript.

Author Contributions

Conceptualization: Sangly P. Srinivas, Prema Padmanabhan.

Formal analysis: Sangly P. Srinivas, Arushi Goyal, Deepti P. Talele, Sanjay Mahadik, P. Pavani Murthy, Sudhir Ranganath, Uday B. Kompella.

Funding acquisition: Sangly P. Srinivas, Rachapalle Reddi Sudhir, Uday B. Kompella, Prema Padmanabhan.

Investigation: Sangly P. Srinivas, Arushi Goyal, Deepti P. Talele, P. Pavani Murthy.

Methodology: Sangly P. Srinivas, Arushi Goyal, Deepti P. Talele, Sanjay Mahadik, Rachapalle Reddi Sudhir, Prema Padmanabhan.

Project administration: Sangly P. Srinivas, Prema Padmanabhan.

Resources: Sangly P. Srinivas, Rachapalle Reddi Sudhir, Uday B. Kompella.

Software: Sangly P. Srinivas.

Supervision: Sangly P. Srinivas, Rachapalle Reddi Sudhir, Uday B. Kompella, Prema Padmanabhan.

Validation: Sangly P. Srinivas.

Writing – original draft: Sangly P. Srinivas.

Writing – review & editing: Sangly P. Srinivas, Arushi Goyal, Deepti P. Talele, Rachapalle Reddi Sudhir, P. Pavani Murthy, Sudhir Ranganath, Uday B. Kompella, Prema Padmanabhan.

References

1. DelMonte DW, Kim T. Anatomy and physiology of the cornea. *Journal of cataract and refractive surgery*. 2011; 37(3):588–98. <https://doi.org/10.1016/j.jcrs.2010.12.037> PMID: 21333881.
2. Hamalainen KM, Kananen K, Auriola S, Kontturi K, Urtti A. Characterization of paracellular and aqueous penetration routes in cornea, conjunctiva, and sclera. *Invest Ophthalmol Vis Sci*. 1997; 38(3):627–34. PMID: 9071216.
3. Urtti A. Challenges and obstacles of ocular pharmacokinetics and drug delivery. *Adv Drug Deliv Rev*. 2006; 58(11):1131–5. <https://doi.org/10.1016/j.addr.2006.07.027> PMID: 17097758.
4. Maurice DM. Factors influencing the penetration of topically applied drugs. *Int Ophthalmol Clin*. 1980; 20(3):21–32. PMID: 6998898.
5. Maurice DM. Prolonged-action drops. *Int Ophthalmol Clin*. 1993; 33(4):81–91. PMID: 8258500.
6. Maurice DM, Mishima S. Ocular Pharmacokinetics. In: Maurice DM, Mishima S, editors. *Pharmacology of the Eye*. 69. New York: Springer Verlag; 1984. p. 19–116.
7. Kinoshita S, Adachi W, Sotozono C, Nishida K, Yokoi N, Quantock AJ, et al. Characteristics of the human ocular surface epithelium. *Prog Retin Eye Res*. 2001; 20(5):639–73. PMID: 11470454.
8. Gaudana R, Ananthula HK, Parenky A, Mitra AK. Ocular drug delivery. *The AAPS journal*. 2010; 12(3):348–60. <https://doi.org/10.1208/s12248-010-9183-3> PMID: 20437123.
9. Pflugfelder SC, Farley W, Luo L, Chen LZ, de Paiva CS, Olmos LC, et al. Matrix metalloproteinase-9 knockout confers resistance to corneal epithelial barrier disruption in experimental dry eye. *Am J Pathol*. 2005; 166(1):61–71. [https://doi.org/10.1016/S0002-9440\(10\)62232-8](https://doi.org/10.1016/S0002-9440(10)62232-8) PMID: 15632000.
10. Kimura K, Teranishi S, Fukuda K, Kawamoto K, Nishida T. Delayed disruption of barrier function in cultured human corneal epithelial cells induced by tumor necrosis factor-alpha in a manner dependent on NF-kappaB. *Invest Ophthalmol Vis Sci*. 2008; 49(2):565–71. <https://doi.org/10.1167/iovs.07-0419> PMID: 18235000.
11. Kimura K, Teranishi S, Nishida T. Interleukin-1beta-induced disruption of barrier function in cultured human corneal epithelial cells. *Invest Ophthalmol Vis Sci*. 2009; 50(2):597–603. <https://doi.org/10.1167/iovs.08-2606> PMID: 19171646.
12. Yokoi N, Komuro A, Maruyama K, Kinoshita S. New instruments for dry eye diagnosis. *Semin Ophthalmol*. 2005; 20(2):63–70. <https://doi.org/10.1080/08820530590931124> PMID: 16020346.

13. Suzuki K, Tanaka T, Enoki M, Nishida T. Coordinated reassembly of the basement membrane and junctional proteins during corneal epithelial wound healing. *Invest Ophthalmol Vis Sci.* 2000; 41(9):2495–500. PMID: [10937559](#).
14. Shimazaki J, Shimmura S, Mochizuki K, Tsubota K. Morphology and barrier function of the corneal epithelium after penetrating keratoplasty: association with original diseases, tear function, and suture removal. *Cornea.* 1999; 18(5):559–64. PMID: [10487430](#).
15. Tanihara H, Yokoi N, Komuro A, Honda Y, Kinoshita S. Prolonged impairment of peripheral corneal epithelium barrier function after successful trabeculectomy. *Am J Ophthalmol.* 1997; 123(4):487–93. PMID: [9124245](#).
16. Hutcheon AE, Sippel KC, Zieske JD. Examination of the restoration of epithelial barrier function following superficial keratectomy. *Exp Eye Res.* 2007; 84(1):32–8. <https://doi.org/10.1016/j.exer.2006.08.011> PMID: [17067576](#).
17. Nejima R, Miyata K, Tanabe T, Okamoto F, Hiraoka T, Kiuchi T, et al. Corneal barrier function, tear film stability, and corneal sensation after photorefractive keratectomy and laser in situ keratomileusis. *Am J Ophthalmol.* 2005; 139(1):64–71. <https://doi.org/10.1016/j.ajo.2004.08.039> PMID: [15652829](#).
18. Polunin GS, Kourenkov VV, Makarov IA, Polunina EG. The corneal barrier function in myopic eyes after laser in situ keratomileusis and after photorefractive keratectomy in eyes with haze formation. *Journal of refractive surgery.* 1999; 15(2 Suppl):S221–4. PMID: [10202726](#).
19. Savitsky DZ, Fan VC, Yildiz EH, Du TT, Asbell PA. Fluorophotometry to evaluate the corneal epithelium in eyes undergoing contact lens corneal reshaping to correct myopia. *Journal of refractive surgery.* 2009; 25(4):366–70. PMID: [19431927](#).
20. Bardag-Gorce F, Hoff RH, Wood A, Oliva J, Niihara H, Makalinalo A, et al. The Role of E-Cadherin in Maintaining the Barrier Function of Corneal Epithelium after Treatment with Cultured Autologous Oral Mucosa Epithelial Cell Sheet Grafts for Limbal Stem Deficiency. *J Ophthalmol.* 2016; 2016:4805986. <https://doi.org/10.1155/2016/4805986> PMID: [27777792](#).
21. Hayashi Y, Toshida H, Matsuzaki Y, Matsui A, Ohta T. Persistent corneal epithelial defect responding to rebamipide ophthalmic solution in a patient with diabetes. *Int Med Case Rep J.* 2016; 9:113–6. <https://doi.org/10.2147/IMCRJ.S103299> PMID: [27257394](#).
22. Gekka M, Miyata K, Nagai Y, Nemoto S, Sameshima T, Tanabe T, et al. Corneal epithelial barrier function in diabetic patients. *Cornea.* 2004; 23(1):35–7. PMID: [14701955](#).
23. Gobbels M, Spitznas M, Oldendoerp J. Impairment of corneal epithelial barrier function in diabetics. *Graefes Arch Clin Exp Ophthalmol.* 1989; 227(2):142–4. PMID: [2721983](#).
24. Chang SW, Hsu HC, Hu FR, Chen MS. Corneal autofluorescence and epithelial barrier function in diabetic patients. *Ophthalmic Res.* 1995; 27(2):74–9. <https://doi.org/10.1159/000267600> PMID: [8538986](#).
25. Ramselaar JA, Boot JP, van Haeringen NJ, van Best JA, Oosterhuis JA. Corneal epithelial permeability after instillation of ophthalmic solutions containing local anaesthetics and preservatives. *Curr Eye Res.* 1988; 7(9):947–50. PMID: [2460291](#).
26. Gobbels M, Spitznas M. Influence of artificial tears on corneal epithelium in dry-eye syndrome. *Graefes Arch Clin Exp Ophthalmol.* 1989; 227(2):139–41. PMID: [2721982](#).
27. McCarey BE, Reaves TA. Effect of tear lubricating solutions on in vivo corneal epithelial permeability. *Curr Eye Res.* 1997; 16(1):44–50. PMID: [9043822](#).
28. Gobbels M, Spitznas M. Effects of artificial tears on corneal epithelial permeability in dry eyes. *Graefes Arch Clin Exp Ophthalmol.* 1991; 229(4):345–9. PMID: [1916322](#).
29. Joshi A, Maurice D, Paugh JR. A new method for determining corneal epithelial barrier to fluorescein in humans. *Investigative ophthalmology & visual science.* 1996; 37(6):1008–16. PMID: [8631616](#).
30. Leung T, Zhou Y, French HM, Lin MC. Increased corneal epithelial permeability after overnight sleep. *Invest Ophthalmol Vis Sci.* 2014; 55(9):5718–22. <https://doi.org/10.1167/iov.14-14259> PMID: [25118261](#).
31. Li WY, Hsiao C, Graham AD, Lin MC. Corneal epithelial permeability: ethnic differences between Asians and non-Asians. *Cont Lens Anterior Eye.* 2013; 36(5):215–8. <https://doi.org/10.1016/j.clae.2013.02.006> PMID: [23507503](#).
32. Lin MC, French HM, Graham AD, Sanders TL. Effects of daily irrigation on corneal epithelial permeability and adverse events with silicone hydrogel contact lens continuous wear. *Invest Ophthalmol Vis Sci.* 2014; 55(2):776–83. <https://doi.org/10.1167/iov.13-13508> PMID: [24425854](#).
33. Lin MC, Polse KA. Hypoxia, overnight wear, and tear stagnation effects on the corneal epithelium: data and proposed model. *Eye Contact Lens.* 2007; 33(6 Pt 2):378–81; discussion 82. <https://doi.org/10.1097/ICL.0b013e318157d7c9> PMID: [17975425](#).

34. Lin MC, Soliman GN, Song MJ, Smith JP, Lin CT, Chen YQ, et al. Soft contact lens extended wear affects corneal epithelial permeability: hypoxic or mechanical etiology? *Cont Lens Anterior Eye*. 2003; 26(1):11–6. [https://doi.org/10.1016/S1367-0484\(02\)00088-7](https://doi.org/10.1016/S1367-0484(02)00088-7) PMID: 16303492.
35. McNamara NA, Chan JS, Han SC, Polse KA, McKenney CD. Effects of hypoxia on corneal epithelial permeability. *Am J Ophthalmol*. 1999; 127(2):153–7. PMID: 10030556.
36. Nelson JD. Simultaneous evaluation of tear turnover and corneal epithelial permeability by fluorophotometry in normal subjects and patients with keratoconjunctivitis sicca (KCS). *Trans Am Ophthalmol Soc*. 1995; 93:709–53. PMID: 8719697.
37. McNamara NA, Fusaro RE, Brand RJ, Polse KA, Srinivas SP. Measurement of corneal epithelial permeability to fluorescein. A repeatability study. *Invest Ophthalmol Vis Sci*. 1997; 38(9):1830–9. PMID: 9286273.
38. Bron AJ, Argueso P, Irkec M, Bright FV. Clinical staining of the ocular surface: mechanisms and interpretations. *Prog Retin Eye Res*. 2015; 44:36–61. <https://doi.org/10.1016/j.preteyeres.2014.10.001> PMID: 25461622.
39. Kasnavia T, Sabaini DA. Fluorescent dye and media properties affecting sorption and tracer selection. *Ground Water*. 1999; 37(3).
40. Oba Y, Poulson SR. Octanol-water partition coefficients (K_{ow}) vs. pH for fluorescent dye tracers (fluorescein, eosin Y), and implications for hydrologic tracer tests. *Geochem J*. 2012; 46(6):517–20.
41. Gupta C, Chauhan A, Srinivas SP. Penetration of fluorescein across the rabbit cornea from the endothelial surface. *Pharm Res*. 2012; 29(12):3325–34. <https://doi.org/10.1007/s11095-012-0824-3> PMID: 22814903.
42. Gupta C, Chauhan A, Mutharasan R, Srinivas SP. Measurement and modeling of diffusion kinetics of a lipophilic molecule across rabbit cornea. *Pharm Res*. 2010; 27(4):699–711. <https://doi.org/10.1007/s11095-010-0066-1> PMID: 20182774.
43. Leong YY, Tong L. Barrier function in the ocular surface: from conventional paradigms to new opportunities. *Ocul Surf*. 2015; 13(2):103–9. <https://doi.org/10.1016/j.jtos.2014.10.003> PMID: 25881994.
44. Brubaker RF, Maurice D, McLaren JW. Fluorometry of the Anterior Segment. In: Masters BR, editor. *Noninvasive Diagnostic Techniques in Ophthalmology*. New York: Springer Verlag; 1990. p. 248–80.
45. Cunha-Vaz JG. The blood-retinal barriers system. Basic concepts and clinical evaluation. *Exp Eye Res*. 2004; 78(3):715–21. PMID: 15106951.
46. Bai Y, Nichols JJ. Advances in thickness measurements and dynamic visualization of the tear film using non-invasive optical approaches. *Prog Retin Eye Res*. 2017; 58:28–44. Epub 2017/03/04. <https://doi.org/10.1016/j.preteyeres.2017.02.002> PMID: 28254520.
47. De Bruyn T, Fattah S, Stieger B, Augustijns P, Annaert P. Sodium fluorescein is a probe substrate for hepatic drug transport mediated by OATP1B1 and OATP1B3. *J Pharm Sci*. 2011; 100(11):5018–30. Epub 2011/08/13. <https://doi.org/10.1002/jps.22694> PMID: 21837650.
48. Mokhtarzadeh M, Casey R, Glasgow BJ. Fluorescein punctate staining traced to superficial corneal epithelial cells by impression cytology and confocal microscopy. *Invest Ophthalmol Vis Sci*. 2011; 52(5):2127–35. Epub 2011/01/08. <https://doi.org/10.1167/iovs.10-6489> PMID: 21212176.
49. Willcox MDP, Argueso P, Georgiev GA, Holopainen JM, Laurie GW, Millar TJ, et al. TFOS DEWS II Tear Film Report. *Ocul Surf*. 2017; 15(3):366–403. Epub 2017/07/25. <https://doi.org/10.1016/j.jtos.2017.03.006> PMID: 28736338.
50. Benedetto DA, Clinch TE, Laibson PR. In vivo observation of tear dynamics using fluorophotometry. *Arch Ophthalmol*. 1984; 102(3):410–2. PMID: 6703990.
51. Brubaker RF, McLaren JW. Uses of fluorophotometry in glaucoma research. *Ophthalmology*. 1985; 92(7):884–90. PMID: 4022573.
52. Fahim MM, Haji S, Koonapareddy CV, Fan VC, Asbell PA. Fluorophotometry as a diagnostic tool for the evaluation of dry eye disease. *BMC Ophthalmol*. 2006; 6:20. <https://doi.org/10.1186/1471-2415-6-20> PMID: 16729882.
53. Jones DP, Webber WR, Smith AT, Lloyd-Jones D, Wright P. Ophthalmic fluorophotometry: a new solid state fluorophotometer. *J Biomed Eng*. 1982; 4(2):113–7. PMID: 7073825.
54. McNamara NA, Polse KA, Bonanno JA. Fluorophotometry in contact lens research: the next step. *Optometry and vision science: official publication of the American Academy of Optometry*. 1998; 75(5):316–22. PMID: 9624695.
55. McCarey BE, al Reaves T. Noninvasive measurement of corneal epithelial permeability. *Curr Eye Res*. 1995; 14(6):505–10. PMID: 7671632.
56. de Kruijf EJ, Boot JP, Laterveer L, van Best JA, Ramselaar JA, Oosterhuis JA. A simple method for determination of corneal epithelial permeability in humans. *Curr Eye Res*. 1987; 6(11):1327–34. PMID: 3427981.

57. Edward A, Prausnitz MR. Predicted permeability of the cornea to topical drugs. *Pharm Res.* 2001; 18(11):1497–508. PMID: [11758755](#).
58. Prausnitz MR, Noonan JS. Permeability of cornea, sclera, and conjunctiva: a literature analysis for drug delivery to the eye. *J Pharm Sci.* 1998; 87(12):1479–88. PMID: [10189253](#).
59. Zhang W, Prausnitz MR, Edwards A. Model of transient drug diffusion across cornea. *J Control Release.* 2004; 99(2):241–58. <https://doi.org/10.1016/j.jconrel.2004.07.001> PMID: [15380634](#).
60. Cunha-Vaz JG. Ocular fluorometry: standardization and instrumentation development. A Concerted Action in the European Community (EUROEYE). *Int Ophthalmol.* 1993; 17(3):147–53. PMID: [8262714](#).
61. Lakowicz JR. *Principles of Fluorescence Spectroscopy*: Springer; 2006.
62. King-Smith PE, Ramamoorthy P, Braun RJ, Nichols JJ. Tear film images and breakup analyzed using fluorescent quenching. *Invest Ophthalmol Vis Sci.* 2013; 54(9):6003–11. <https://doi.org/10.1167/iovs.13-12628> PMID: [23920365](#).
63. Braun RJ, King-Smith PE, Begley CG, Li L, Gewecke NR. Dynamics and function of the tear film in relation to the blink cycle. *Prog Retin Eye Res.* 2015; 45:132–64. <https://doi.org/10.1016/j.preteyeres.2014.11.001> PMID: [25479602](#).
64. van Best JA, Diestelhorst M, Leite E, Fantaguzzi S, Schalmus R. Corneal endothelial permeability and aqueous humor flow using a standard protocol. *Graefes Arch Clin Exp Ophthalmol.* 1995; 233(9):582–91. PMID: [8543210](#).
65. Carlson KH, Bourne WM, McLaren JW, Brubaker RF. Variations in human corneal endothelial cell morphology and permeability to fluorescein with age. *Exp Eye Res.* 1988; 47(1):27–41. Epub 1988/07/01. PMID: [3409985](#).
66. Bradley JS, Garonzik SM, Forrest A, Bhavnani SM. Pharmacokinetics, pharmacodynamics, and Monte Carlo simulation: selecting the best antimicrobial dose to treat an infection. *Pediatr Infect Dis J.* 2010; 29(11):1043–6. Epub 2010/10/27. <https://doi.org/10.1097/INF.0b013e3181f42a53> PMID: [20975453](#).
67. Dokoumetzidis A, Kosmidis K, Argyrakos P, Macheras P. Modeling and Monte Carlo simulations in oral drug absorption. *Basic Clin Pharmacol Toxicol.* 2005; 96(3):200–5. Epub 2005/03/01. <https://doi.org/10.1111/j.1742-7843.2005.pto960309.x> PMID: [15733215](#).
68. Roberts JA, Kirkpatrick CM, Lipman J. Monte Carlo simulations: maximizing antibiotic pharmacokinetic data to optimize clinical practice for critically ill patients. *J Antimicrob Chemother.* 2011; 66(2):227–31. Epub 2010/12/02. <https://doi.org/10.1093/jac/dkq449> PMID: [21118912](#).
69. Gray JR, Mosier MA, Ishimoto BM. Optimized protocol for Fluorotron Master. *Graefes Arch Clin Exp Ophthalmol.* 1985; 222(4–5):225–9. Epub 1985/01/01. PMID: [3979849](#).
70. Munnerlyn CR, Gray JR, Hennings DR. Design considerations for a fluorophotometer for ocular research. *Graefes Arch Clin Exp Ophthalmol.* 1985; 222(4–5):209–11. Epub 1985/01/01. PMID: [3979845](#).
71. Maurice DM, Srinivas SP. Use of fluorometry in assessing the efficacy of a cation-sensitive gel as an ophthalmic vehicle: comparison with scintigraphy. *J Pharm Sci.* 1992; 81(7):615–9. PMID: [1403690](#).
72. Mun EA, Morrison PW, Williams AC, Khutoryanskiy VV. On the barrier properties of the cornea: a microscopy study of the penetration of fluorescently labeled nanoparticles, polymers, and sodium fluorescein. *Mol Pharm.* 2014; 11(10):3556–64. Epub 2014/08/29. <https://doi.org/10.1021/mp500332m> PMID: [25165886](#).
73. Srinivas SP, Maurice DM. A microfluorometer for measuring diffusion of fluorophores across the cornea. *IEEE Trans Biomed Eng.* 1992; 39(12):1283–91. <https://doi.org/10.1109/10.184704> PMID: [1487291](#).
74. Srinivas SP. In situ measurement of fluorescein release by collagen shields in human eyes. *Curr Eye Res.* 1994; 13(4):281–8. PMID: [7518372](#).
75. Yeh TN, Green HM, Zhou Y, Pitts J, Kitamata-Wong B, Lee S, et al. Short-term effects of overnight orthokeratology on corneal epithelial permeability and biomechanical properties. *Invest Ophthalmol Vis Sci.* 2013; 54(6):3902–11. <https://doi.org/10.1167/iovs.13-11874> PMID: [23652492](#).
76. Boot JP, van Best JA, Stolwijk TR, Sterk CC. Epithelial permeability in corneal grafts by fluorophotometry. *Graefes Arch Clin Exp Ophthalmol.* 1991; 229(6):533–5. PMID: [1765293](#).
77. Boets EP, van Best JA, Boot JP, Oosterhuis JA. Corneal epithelial permeability and daily contact lens wear as determined by fluorophotometry. *Curr Eye Res.* 1988; 7(5):511–4. PMID: [3409717](#).
78. Benitez-del-Castillo JM, Aranguiz C, Garcia-Sanchez J. Corneal epithelial permeability and dry eye treatment. *Advances in experimental medicine and biology.* 2002; 506(Pt A):703–6. PMID: [12613980](#).
79. Li Y, Liu J, Pan D, Hopfinger AJ. A study of the relationship between cornea permeability and eye irritation using membrane-interaction QSAR analysis. *Toxicol Sci.* 2005; 88(2):434–46. <https://doi.org/10.1093/toxsci/kfi319> PMID: [16162848](#).